Springer book chapter manuscript No.
(will be inserted by the editor)

Nowcasting of COVID-19 confirmed cases: Foundations, trends, and challenges

Tanujit Chakraborty · Indrajit Ghosh · Tirna Mahajan · Tejasvi Arora

Received: date / Accepted: date

Abstract The coronavirus disease 2019 (COVID-19) has become a public health emergency of international concern affecting more than 200 countries and territories worldwide. As of September 30, 2020, it has caused a pandemic outbreak with more than 33 million confirmed infections, and more than 1 million reported deaths worldwide. Several statistical, machine learning, and hybrid models have previously been applied to forecast COVID-19 confirmed cases for profoundly affected countries. Future predictions of daily COVID-19 cases are useful for the effective allocation of healthcare resources and will act as an early-warning system for government policymakers. However, due to the presence of extreme uncertainty in these time series datasets, forecasting of COVID-19 confirmed cases has become a very challenging job. For univariate time series forecasting, there are various statistical and machine learning models available in the literature. Still, nowcasting and forecasting of COVID-19 cases are difficult due to insufficient input data, flaw in modeling assumptions, lack of epidemiological features, inadequate past evidence on effects of available interventions, and lack of transparency. This chapter focuses on assessing different short-term forecasting models that are popularly used to forecast the daily COVID-19 cases for various countries. This chapter provides strong empirical evidence that there is no universal method available that can accurately forecast pandemic data.

Keywords Coronavirus disease; Statistical models; Machine learning models; Hybrid models; Forecasting.

1 Introduction

In December 2019, clusters of pneumonia cases caused by the novel Coronavirus (COVID-19) were identified at the Wuhan, Hubei province in China (Huang et al, 2020; Guan et al, 2020) after almost a hundred years of the 1918 Spanish flu (Trilla et al, 2008). Soon after the emergence of the novel beta coronavirus, World Health Organization (WHO) characterized this contagious disease as a "global pandemic" due to its rapid spread worldwide (Roosa et al, 2020). Many scientists have attempted to make forecasts about its impact. However, despite involving many excellent modelers, best intentions, and highly sophisticated tools, forecasting COVID-19 pandemics is harder (Ioannidis et al, 2020), and this is primarily due to the following major factors: (a) Very less amount of data is available; (b) Less understanding of the factors that contribute to it; (c) Model accuracy is constrained by

Indian Statistical Institute, 203, B.T. Road, Kolkata - 700108, West Bengal, India
Corresponding Author's Email: indra7math@gmail.com

our knowledge of the virus, however. With an emerging disease such as COVID-19, many transmission-related biologic features are hard to measure and remain unknown; (d) The most obvious source of uncertainty affecting all models is that we don't know how many people are or have been infected; (e) Ongoing issues with virologic testing mean that we are certainly missing a substantial number of cases, so models fitted to confirmed cases are likely to be highly uncertain (Holmdahl and Buckee, 2020); (f) The problem of using confirmed cases to fit models is further complicated because the fraction of confirmed cases is spatially heterogeneous and time-varying (Weinberger et al, 2020); and (g) Finally, many parameters associated with COVID-19 transmission are poorly understood.

Amid enormous uncertainty about the future of the COVID-19 pandemic, statistical, machine learning, and epidemiological models are critical forecasting tools for policymakers, clinicians, and public health practitioners (Chakraborty and Ghosh, 2020; Li et al, 2020; Wu et al, 2020; Fanelli and Piazza, 2020; Kucharski et al, 2020; Zhuang et al, 2020). COVID-19 modeling studies generally follow one of two general approaches that we will refer to as forecasting models and mechanistic models. Although there are hybrid approaches, these two model types tend to address different questions on different time scales, and they deal differently with uncertainty (Ghosh and Chakraborty, 2020). Compartmental epidemiological models have been developed over nearly a century and are well tested on data from past epidemics. These models are based on modeling the actual infection process and are useful for predicting long-term trajectories of the epidemic curves (Ghosh and Chakraborty, 2020). Short-term Forecasting models are often statistical, fitting a line or curve to data and extrapolating from there – like seeing a pattern in a sequence of numbers and guessing the next number, without incorporating the process that produces the pattern (Chakraborty et al, 2020, 2019; Chakraborty and Ghosh, 2020). Well constructed statistical frameworks can be used for short-term forecasts, using machine learning or regression. In statistical models, the uncertainty of the prediction is generally presented as statistically computed prediction intervals around an estimate (Hastie et al, 2009; James et al, 2013). Given that what happens a month from now will depend on what happens in the interim, the estimated uncertainty should increase as you look further into the future. These models yield quantitative projections that policymakers may need to allocate resources or plan interventions in the short-term.

Forecasting time series datasets have been a traditional research topic for decades, and various models have been developed to improve forecasting accuracy (Chatfield, 2000; Armstrong, 2001; Hanke et al, 2001). There are numerous methods available to forecast time series, including traditional statistical models and machine learning algorithms, providing many options for modelers working on epidemiological forecasting (Chakraborty et al, 2019; Ghosh and Chakraborty, 2020; Brady et al, 2012; Chakraborty and Ghosh, 2020; Messina et al, 2014; Buczak et al, 2018; Ribeiro et al, 2020). Many research efforts have focused on developing a universal forecasting model but failed, which is also evident from the "No Free Lunch Theorem" (Wolpert and Macready, 1997). This chapter focuses on assessing popularly used short-term forecasting (nowcasting) models for COVID-19 from an empirical perspective. The findings of this chapter will fill the gap in the literature of the nowcasting of COVID-19 by comparing various forecasting methods, understanding global characteristics of pandemic data, and discovering real challenges for pandemic forecasters.

This chapter is organized as follows: in Section 2, we present a collection of recent findings on COVID-19 forecasting. Some global characteristics of time series data are outlined in Section 3. Several nowcasting models from statistical, machine learning and hybrid algorithms are described in Section 4. Section 5 reports the experimental results for the

United States of America (USA), India, Brazil, Russia, and Peru data sets. In Section 6, the experimental findings are briefly discussed. Finally, in Section 7, some recommendations for policy-making decisions and limitations of these forecasting tools have been presented.

2 Related works

Researchers face unprecedented challenges during this global pandemic to forecast future real-time cases with traditional mathematical, statistical, forecasting, and machine learning tools (Li et al, 2020; Wu et al, 2020; Fanelli and Piazza, 2020; Kucharski et al, 2020; Zhuang et al, 2020). Studies in March with simple yet powerful forecasting methods like the exponential smoothing model predicted cases ten days ahead that, despite the positive bias, had reasonable forecast error (Petropoulos and Makridakis, 2020). Early linear and exponential model forecasts for better preparation regarding hospital beds, ICU admission estimation, resource allocation, emergency funding, and proposing strong containment measures were conducted (Grasselli et al, 2020) that projected about 869 ICU and 14542 ICU admissions in Italy for March 20, 2020. Health-care workers had to go through immense mental stress left with a formidable choice of prioritizing young and healthy adults over the elderly for allocation of life support, mostly unwanted ignoring of those who are extremely unlikely to survive (Emanuel et al, 2020; Rosenbaum, 2020). Real estimates of mortality with 14-days delay demonstrated underestimating of the COVID-19 outbreak and indicated a grave future with a global case fatality rate (CFR) of 5.7% in March (Baud et al, 2020). The contact tracing, quarantine, and isolation efforts have a differential effect on the mortality due to COVID-19 among countries. Even though it seems that the CFR of COVID-19 is less compared to other deadly epidemics, there are concerns about it being eventually returning as the seasonal flu, causing a second wave or future pandemic (Petersen et al, 2020; Rajgor et al, 2020).

Mechanistic models, like the Susceptible–Exposed–Infectious–Recovered (SEIR) frameworks, try to mimic the way COVID-19 spreads and are used to forecast or simulate future transmission scenarios under various assumptions about parameters governing the transmission, disease, and immunity (Hou et al, 2020; He et al, 2020; Annas et al, 2020; Chen et al, 2020; López and Rodó, 2020). Mechanistic modeling is one of the only ways to explore possible long-term epidemiologic outcomes (Anderson et al, 1992). For example, the model from Ferguson et al (2020) that has been used to guide policy responses in the United States and Britain examines how many COVID-19 deaths may occur over the next two years under various social distancing measures. Kissler et al (2020) ask whether we can expect seasonal, recurrent epidemics if immunity against novel coronavirus functions similarly to immunity against the milder coronaviruses that we transmit seasonally. In a detailed mechanistic model of Boston-area transmission, Aleta et al (2020) simulate various lockdown "exit strategies". These models are a way to formalize what we know about viral transmission and explore possible futures of a system that involves nonlinear interactions, which is almost impossible to do using intuition alone (Hellewell et al, 2020; Mossong et al, 2008). Although these epidemiological models are useful for estimating the dynamics of transmission, targeting resources, and evaluating the impact of intervention strategies, the models require parameters and depend on many assumptions.

Several statistical and machine learning methods for real-time forecasting of the new and cumulative confirmed cases of COVID-19 are developed to overcome limitations of the epidemiological model approaches and assist public health planning and policy-making (Ghosh and Chakraborty, 2020; Petropoulos and Makridakis, 2020; Anastassopoulou et al,

2020; Chakraborty and Ghosh, 2020; Chakraborty et al, 2020). Real-time forecasting with foretelling predictions is required to reach a statistically validated conjecture in this current health crisis. Some of the leading-edge research concerning real-time projections of COVID-19 confirmed cases, recovered cases, and mortality using statistical, machine learning, and mathematical time series modeling are given in Table 1.

Table 1 Related works on nowcasting and forecasting of COVID-19 pandemic

Research Topic	Date	Countries	Model	Results	Main Conclusion
Forecasting and risk assessment (Chakraborty and Ghosh, 2020)	January 30-31, 2020, to April 4, 2020	Canada, France, India, South Korea, UK	ARIMA,Wavelet ARIMA(WBF), Hybrid ARIMA-WBF	MAE and RMSE least for Hybrid ARIMA-WBF	Hybrid ARIMA-WBF performs better than traditional methods and important factors that impact on case fatality rates are estimated using regression tree.
Forecasting the confirmed and recovered cases (Maleki et al, 2020)	Jan 22,2020 to April 30, 2020	World data	TP–SMN–AR time series (Autoregressive series based on two-piece scale mixture normal distributions)	MAPE = 0.22 for confirmed cases; MAPE = 1.6 for Recovered cases	Provided reasonable forecasts in terms of error and model selection.
Short-term forecasting of cumulative confirmed cases (Ribeiro et al, 2020)	Inception - April 18-19, 2020	Brazil	ARIMA, Random forest, Ridge regression, Support vector regression, Ensemble learning	Forecast errors lower than 6.9 percent	SVR and stacking-ensemble learning model are suitable tools for forecasting COVID-19.
Modelling and forecasting daily cases (Anastassopoulou et al, 2020)	January 11 to February 10, 2020	China	Susceptible-Infectious-Recovered-Dead (SIRD) model	Estimated average reproduction number (R_0) 2.6 and CFR 0.15%	simulations predicted a decline of the outbreak at the end of February.
Forecasting COVID-19 (Petropoulos and Makridakis, 2020)	January 22, 2020 to March 11, 2020	Global data	Exponential smoothing models	Ten-days-ahead forecasts have actual cases within 90% CI	Forecasts reflect the significant increase in the trend of global cases with growing uncertainty.
Real-time forecasting (Roosa et al, 2020)	February 5to February 24, 2020	China	Generalized logistic growth model (GLM) and Sub-epidemic wave model	Mean case estimates and 95% prediction intervals emulsifies the global picture 15-days ahead	All methods perform similarly and and increase in data inclusion decreases the width of prediction intervals.
Predictions and role of interventions (Ray et al, 2020)	Live forecast	India	Extended state-space SIR epidemiological models	Live forecasts with broad confidence intervals	Lockdown has a high chance of reducing the number of COVID-19 cases.
Forecasting and nowcasting COVID-19 (Wu et al, 2020)	Dec 31, 2019, to Jan 28, 2020	China	Susceptible-exposed-infectious-recovered (SEIR) model	R_0 = 2.68 (95% CI 2.47, 2.86) ; Epidemic doubling time = 6.4 days (95% CI 5.8, 7.1)	COVID-19 is no longer contained within China, and human-human transmission became evident.
Forecast (Fanelli and Piazza, 2020)	Jan, 22- March 15, 2020	China, Italy and France	Susceptible, infected, recovered, dead (SIRD) model	The recovery rate is the same for Italy and China, while infection and death rate appear to be different.	There is a certain universality in the time evolution of COVID-19.
AI-based forecasts (Hu et al, 2020)	Jan, 11 - February 27, 2020	China	Data driven AI-based methods	Using the multiple-step forecasting, forecasts are given till April 19, 2020 for 34 provinces/cities.	The accuracy of the AI-based methods for forecasting the trajectory of COVID-19 was high.
Machine learning-based forecasts (Sujath et al, 2020)	January 22, 2020, to April 10, 2020	India	Multi-layered perceptron (MLP) model	Forecast of confirmed, deaths and recovered cases for 69 days	MLP method is giving good prediction results than other methods.
Long-term trajectories of COVID-19 (Ghosh and Chakraborty, 2020)	Starting - June 17, 2020	Spain and Italy	Integrated stochastic-deterministic (ISA) approach	Basic reproduction number and estimated future cases are computed.	ISA model shows significant improvement in the long-term forecasting of COVID-19 cases.

3 Global characteristics of pandemic time series

A univariate time series is the simplest form of temporal data and is a sequence of real numbers collected regularly over time, where each number represents a value (Chatfield, 2016; Box et al, 2015). There are broadly two major steps involved in univariate time series forecasting (Hyndman and Athanasopoulos, 2018): (a) Studying the global characteristics of the time series data; and (b) Analysis of data with the 'best-fitted' forecasting model.

Understanding the global characteristics of pandemic confirmed cases data can help forecasters determine what kind of forecasting method will be appropriate for the given situation (Tsay, 2000). As such, we aim to perform a meaningful data analysis, including the study of time series characteristics, to provide a suitable and comprehensive knowledge foundation for the future step of selecting an apt forecasting method. Thus, we take the path of using statistical measures to understand pandemic time series characteristics to assist method selection and data analysis. These characteristics will carry summarized information of the time series, capturing the 'global picture' of the datasets. Based on the recommendation of De Gooijer and Hyndman (2006); Wang et al (2009); Lemke and Gabrys (2010); Lemke et al (2015), we study several classical and advanced time series characteristics of COVID-19 data. This study considers eight global characteristics of the time series: periodicity, stationarity, serial correlation, skewness, kurtosis, nonlinearity, long-term dependence, and chaos. This collection of measures provides quantified descriptions and gives a rich portrait of the pandemic time-series' nature. A brief description of these statistical and advanced time-series measures are given below.

3.1 Periodicity

A seasonal pattern exists when a time series is influenced by seasonal factors, such as the month of the year or day of the week. The seasonality of a time series is defined as a pattern that repeats itself over fixed intervals of time (Box et al, 2015). In general, the seasonality can be found by identifying a large autocorrelation coefficient or a large partial autocorrelation coefficient at the seasonal lag. Since the periodicity is very important for determining the seasonality and examining the cyclic pattern of the time series, the periodicity feature extraction becomes a necessity. Unfortunately, many time series available from the dataset in different domains do not always have known frequency or regular periodicity. Seasonal time series are sometimes also called cyclic series, although there is a significant distinction between them. Cyclic data have varying frequency lengths, but seasonality is of a fixed length over each period. For time series with no seasonal pattern, the frequency is set to 1. The seasonality is tested using the 'stl' function within the "stats" package in R statistical software (Hyndman and Athanasopoulos, 2018).

3.2 Stationarity

Stationarity is the foremost fundamental statistical property tested for in time series analysis because most statistical models require that the underlying generating processes be stationary (Chatfield, 2000). Stationarity means that a time series (or rather the process rendering it) do not change over time. In statistics, a unit root test tests whether a time series variable is non-stationary and possesses a unit root (Phillips and Perron, 1988). The null hypothesis is generally defined as the presence of a unit root, and the alternative hypothesis is either stationarity, trend stationarity, or explosive root depending on the test used. In econometrics, Kwiatkowski–Phillips–Schmidt–Shin (KPSS) tests are used for

testing a null hypothesis that an observable time series is stationary around a deterministic trend (that is, trend-stationary) against the alternative of a unit root (Shin and Schmidt, 1992). The KPSS test is done using the 'kpss.test' function within the "tseries" package in R statistical software (Trapletti et al, 2007).

3.3 Serial correlation

Serial correlation is the relationship between a variable and a lagged version of itself over various time intervals. Serial correlation occurs in time-series studies when the errors associated with a given time period carry over into future time periods (Box et al, 2015). We have used Box-Pierce statistics (Box and Pierce, 1970) in our approach to estimate the serial correlation measure and extract the measures from COVID-19 data. The Box-Pierce statistic was designed by Box and Pierce in 1970 for testing residuals from a forecast model (Wang et al, 2009). It is a common portmanteau test for computing the measure. The mathematical formula of the Box-Pierce statistic is as follows:

$$Q_h = n \sum_{k=1}^{h} r_k^2, \tag{1}$$

where n is the length of the time series, h is the maximum lag being considered (usually h is chosen as 20), and r_k is the autocorrelation function. The portmanteau test is done using the 'Box.test' function within the "stats" package in R statistical software (Hyndman et al, 2007).

3.4 Nonlinearity

Nonlinear time series models have been used extensively to model complex dynamics not adequately represented by linear models (Kantz and Schreiber, 2004). Nonlinearity is one important time series characteristic to determine the selection of an appropriate forecasting method (Tong, 2002). There are many approaches to test the nonlinearity in time series models, including a nonparametric kernel test and a Neural Network test (Tsay, 1986). In the comparative studies between these two approaches, the Neural Network test has been reported with better reliability (Wang et al, 2009). In this research, we used Teräsvirta's neural network test (Teräsvirta et al, 1993) for measuring time series data nonlinearity. It has been widely accepted and reported that it can correctly model the nonlinear structure of the data (Teräsvirta et al, 2005). It is a test for neglected nonlinearity, likely to have power against a range of alternatives based on the NN model (augmented single-hidden-layer feedforward neural network model). This takes large values when the series is nonlinear and values near zero when the series is linear. The test is done using the 'nonlinearityTest' function within the "nonlinearTseries" package in R statistical software (Garcia and Sawitzki, 2015).

3.5 Skewness

Skewness is a measure of symmetry, or more precisely, the lack of symmetry. A distribution, or dataset, is symmetric if it looks the same to the left and the right of the center point (Wang et al, 2009). A skewness measure is used to characterize the degree of asymmetry

of values around the mean value (Mood, 1950). For univariate data Y_t, the skewness coefficient is

$$S = \frac{1}{n\sigma^3} \sum_{t=1}^{n} \left(Y_t \quad \bar{Y}\right)^3, \tag{2}$$

where $\bar{Y}$ is the mean, σ is the standard deviation, and n is the number of data points. The skewness for a normal distribution is zero, and any symmetric data should have the skewness near zero. Negative values for the skewness indicate data that are skewed left, and positive values for the skewness indicate data that are skewed right. In other words, left skewness means that the left tail is heavier than the right tail. Similarly, right skewness means the right tail is heavier than the left tail (Kim, 2013). Skewness is calculated using the 'skewness' function within the "e1071" package in R statistical software (Meyer et al, 2019).

3.6 Kurtosis (heavy-tails)

Kurtosis is a measure of whether the data are peaked or flat, relative to a normal distribution (Mood, 1950). A dataset with high kurtosis tends to have a distinct peak near the mean, decline rather rapidly, and have heavy tails. Datasets with low kurtosis tend to have a flat top near the mean rather than a sharp peak. For a univariate time series Y_t, the kurtosis coefficient is $\frac{1}{n\sigma^4} \sum_{t=1}^{n} \left(Y_t \quad \bar{Y}\right)^4$. The kurtosis for a standard normal distribution is 3. Therefore, the excess kurtosis is defined as

$$K = \frac{1}{n\sigma^4} \sum_{t=1}^{n} \left(Y_t \quad \bar{Y}\right)^4 \quad 3. \tag{3}$$

So, the standard normal distribution has an excess kurtosis of zero. Positive kurtosis indicates a 'peaked' distribution and negative kurtosis indicates a 'flat' distribution (Groeneveld and Meeden, 1984). Kurtosis is calculated using the 'kurtosis' function within the "PerformanceAnalytics" package in R statistical software (Peterson et al, 2018).

3.7 Long-range Dependence

Processes with long-range dependence have attracted a good deal of attention from a probabilistic perspective in time series analysis (Robinson, 1995). With such increasing importance of the 'self-similarity' or 'long-range dependence' as one of the time series characteristics, we study this feature into the group of pandemic data characteristics. The definition of self-similarity is most related to the self-similarity parameter, also called Hurst exponent (H) (Black et al, 1965). The class of autoregressive fractionally integrated moving average (ARFIMA) processes (Granger and Joyeux, 1980) is a good estimation method for computing H. In an ARIMA(p, d, q), p is the order of AR, d is the degree first differencing involved, and q is the order of MA. If the time series is suspected of exhibiting long-range dependency, parameter d may be replaced by certain non-integer values in the ARFIMA model (Brockwell et al, 1991). We fit an ARFIMA$(0, d, 0)$ to the maximum likelihood, which is approximated by using the fast and accurate method of Haslett and Raftery (Haslett and Raftery, 1989). We then estimate the Hurst parameter using the relation $H = d + 0.5$. The self-similarity feature can only be detected in the RAW data of the time series. The value of H can be obtained using the 'hurstexp' function within the "pracma" package in R statistical software (Borchers and Borchers, 2019).

3.8 Chaos (dynamic systems)

Many systems in nature that were previously considered random processes are now categorized as chaotic systems. For several years, Lyapunov Characteristic Exponents are of interest in the study of dynamical systems to characterize quantitatively their stochasticity properties, related essentially to the exponential divergence of nearby orbits (Farmer and Sidorowich, 1987). Nonlinear dynamical systems often exhibit chaos, characterized by sensitive dependence on initial values, or more precisely by a positive Lyapunov Exponent (LE) (Farmer, 1982). Recognizing and quantifying chaos in time series are essential steps toward understanding the nature of random behavior and revealing the extent to which short-term forecasts may be improved (Hegger et al, 1999). LE, as a measure of the divergence of nearby trajectories, has been used to qualifying chaos by giving a quantitative value (Benettin et al, 1980). The algorithm of computing LE from time-series is applied to continuous dynamical systems in an n-dimensional phase space (Rosenstein et al, 1993). LE is calculated using the 'Lyapunov exponent' function within the "tseriesChaos" package in R statistical software (Antonio et al, 2013).

4 Popular forecasting methods for pandemic nowcasting

Time series forecasting models work by taking a series of historical observations and extrapolating future patterns. These are great when the data are accurate; the future is similar to the past. Forecasting tools are designed to predict possible future alternatives and help current planing and decision making (Armstrong, 2001). There are essentially three general approaches to forecasting a time series (Montero-Manso et al, 2020): 1. Generating forecasts from an individual model; 2. Combining forecasts from many models (forecast model averaging); and 3. Hybrid experts for time series forecasting.

Single (individual) forecasting models are either traditional statistical methods or modern machine learning tools. We study ten popularly used single forecasting models from classical time series, advanced statistics, and machine learning literature. There has been a vast literature on the forecast combinations motivated by the seminal work of Bates & Granger (Bates and Granger, 1969) and followed by a plethora of empirical applications showing that combination forecasts are often superior to their counterparts (see Bordley (1982); Timmermann (2006), for example). Combining forecasts using a weighted average is considered a successful way of hedging against the risk of selecting a misspecified model (Clemen, 1989). A significant challenge is in choosing an appropriate set of weights, and many attempts to do this have been worse than simply using equal weights – something that has become known as the "forecast combination puzzle" (see Smith and Wallis (2009)). To overcome this, hybrid models became popular with the seminal work of Zhang (2003) and further extended for epidemic forecasting in Chakraborty et al (2019); Chakraborty and Ghosh (2020); Chakraborty et al (2020). The forecasting methods can be briefly reviewed and organized in the architecture shown in Figure 1.

4.1 Autoregressive integrated moving average (ARIMA) model

The autoregressive integrated moving average (ARIMA) is one of the well-known linear models in time-series forecasting, developed in the early 1970s (Box et al, 2015). It is widely used to track linear tendencies in stationary time-series data. It is denoted by ARIMA(p, d, q), where the three components have significant meanings. The parameters p and q represent the order of AR and MA models, respectively, and d denotes the level

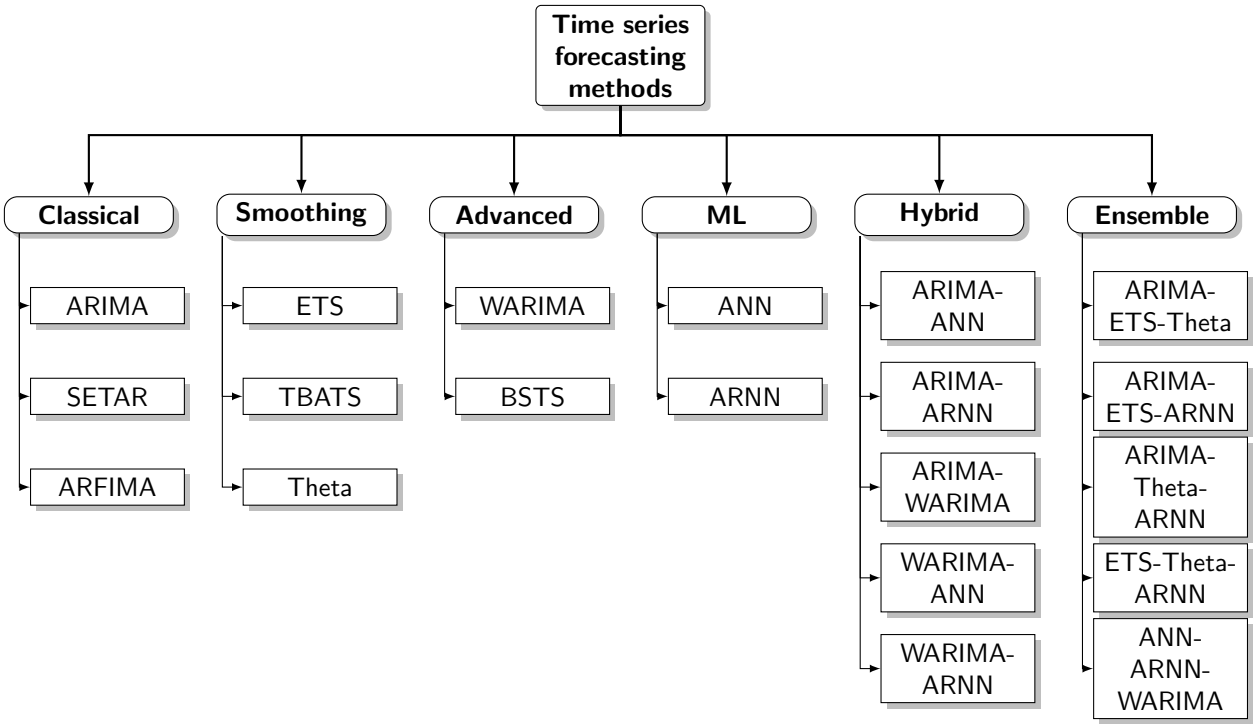

Fig. 1 A systemic view of the various forecasting methods to be used in this study

of differencing to convert nonstationary data into stationary time series (Makridakis and Hibon, 1997). ARIMA model can be mathematically expressed as follows:

$$y_t = \alpha_0 + \sum_{i=1}^{p} \beta_i y_{t\ \ i} + \epsilon_t \quad \sum_{j=1}^{q} \alpha_j \epsilon_{t\ \ j}, \tag{4}$$

where y_t denotes the actual value of the variable at time t, ϵ_t denotes the random error at time t, β_i and α_j are the coefficients of the model. Some necessary steps to be followed for any given time-series dataset to build an ARIMA model are as follows:

- Identification of the model (achieving stationarity).
- Use autocorrelation function (ACF) and partial ACF plots to select the AR and MA model parameters, respectively, and finally estimate model parameters for the ARIMA model.
- The 'best-fitted' forecasting model can be found using the Akaike Information Criteria (AIC) or the Bayesian Information Criteria (BIC). Finally, one checks the model diagnostics to measure its performance.

An implementation in R statistical software is available using the 'auto.arima' function under the "forecast" package, which returns the 'best' ARIMA model according to either AIC or BIC values (Hyndman et al, 2020).

4.2 Wavelet-based ARIMA (WARIMA) model

Wavelet analysis is a mathematical tool that can reveal information within the signals in both the time and scale (frequency) domains. This property overcomes the primary

drawback of Fourier analysis, and wavelet transforms the original signal data (especially in the time domain) into a different domain for data analysis and processing. Wavelet-based models are most suitable for nonstationary data, unlike standard ARIMA. Most epidemic time-series datasets are nonstationary; therefore, wavelet transforms are used as a forecasting model for these datasets (Chakraborty and Ghosh, 2020). When conducting wavelet analysis in the context of time series analysis (Aminghafari and Poggi, 2007), the selection of the optimal number of decomposition levels is vital to determine the performance of the model in the wavelet domain. The following formula for the number of decomposition levels, $WL = int[log(n)]$, is used to select the number of decomposition levels, where n is the time-series length.

The wavelet-based ARIMA (WARIMA) model transforms the time series data by using a hybrid maximal overlap discrete wavelet transform (MODWT) algorithm with a 'haar' filter (Percival and Walden, 2000). Daubechies wavelets can produce identical events across the observed time series in so many fashions that most other time series prediction models cannot recognize. The necessary steps of a wavelet-based forecasting model, defined by Aminghafari and Poggi (2007), are as follows. Firstly, the Daubechies wavelet transformation and a decomposition level are applied to the nonstationary time series data. Secondly, the series is reconstructed by removing the high-frequency component, using the wavelet denoising method. Lastly, an appropriate ARIMA model is applied to the reconstructed series to generate out-of-sample forecasts of the given time series data. Wavelets were first considered as a family of functions by Morlet (Wang, 2002), constructed from the translations and dilation of a single function, which is called "Mother Wavelet". These wavelets are defined as follows:

$$\phi_{m,n}(t) = \frac{1}{\sqrt{jmj}}\phi\left(\frac{t \quad n}{m}\right); \quad m, n \; 2 \; R, \tag{5}$$

where the parameter m ($6=$ 0) is denoted as the scaling parameter or scale, and it measures the degree of compression. The parameter n is used to determine the time location of the wavelet, and it is called the translation parameter. If the value $jmj < 1$, then the wavelet in m is a compressed version (smaller support is the time domain) of the mother wavelet and primarily corresponds to higher frequencies, and when $jmj > 1$, then $\phi_(m, n)(t)$ has larger time width than $\phi(t)$ and corresponds to lower frequencies. Hence wavelets have time width adopted to their frequencies, which is the main reason behind the success of the Morlet wavelets in signal processing and time-frequency signal analysis (Nury et al, 2017). An implementation of the WARIMA model is available using the 'WaveletFittingarma' function under the "WaveletArima" package in R statistical software (Paul et al, 2017).

4.3 Autoregressive fractionally integrated moving average (ARFIMA) model

Fractionally autoregressive integrated moving average or autoregressive fractionally integrated moving average models are the generalized version ARIMA model in time series forecasting, which allow non-integer values of the differencing parameter (Granger and Joyeux, 1980). It may sometimes happen that our time-series data is not stationary, but when we try differencing with parameter d taking the value to be an integer, it may over difference it. To overcome this problem, it is necessary to difference the time series data using a fractional value. These models are useful in modeling time series, which has deviations from the long-run mean decay more slowly than an exponential decay; these models can deal with time-series data having long memory (Pumi et al, 2019). ARFIMA models

can be mathematically expressed as follows:

$$\left(1 \quad \sum_{i=1}^{p} \Phi_i B^i\right)(1 \quad B)^d X_t = \left(1 + \sum_{i=1}^{q} \theta_i B^i\right) \epsilon_t, \tag{6}$$

where B is is the backshift operator, p, q are ARIMA parameters, and d is the differencing term (allowed to take non-integer values). An R implementation of ARFIMA model can be done with 'arfima' function under the "forecast"package (Hyndman et al, 2020). An ARFIMA(p, d, q) model is selected and estimated automatically using the algorithm by Hyndman et al (2008) which can select p and q and the algorithm by Haslett and Raftery (1989) can estimate the parameter d.

4.4 Exponential smoothing state space (ETS) model

Exponential smoothing state space methods are very effective methods in case of time series forecasting. Exponential smoothing was proposed in the late 1950s (Winters, 1960) and has motivated some of the most successful forecasting methods. Forecasts produced using exponential smoothing methods are weighted averages of past observations, with the weights decaying exponentially as the observations get older. The ETS models belong to the family of state-space models, consisting of three-level components such as an error component (E), a trend component (T), and a seasonal component(S). This method is used to forecast univariate time series data. Each model consists of a measurement equation that describes the observed data, and some state equations that describe how the unobserved components or states (level, trend, seasonal) change over time (Hyndman and Athanasopoulos, 2018). Hence, these are referred to as state-space models. The flexibility of the ETS model lies in its ability to trend and seasonal components of different traits. Errors can be of two types: Additive and Multiplicative. Trend Component can be any of the following: None, Additive, Additive Damped, Multiplicative and Multiplicative Damped. Seasonal Component can be of three types: None, Additive, and Multiplicative. Thus, there are 15 models with additive errors and 15 models with multiplicative errors. To determine the best model of 30 ETS models, several criteria such as Akaike's Information Criterion (AIC), Akaike's Information Criterion correction (AICc), and Bayesian Information Criterion (BIC) can be used (Hyndman et al, 2008). An R implementation of the model is available in the 'ets' function under "forecast" package (Hyndman et al, 2020).

4.5 Self-exciting threshold autoregressive (SETAR) model

As an extension of autoregressive model, Self-exciting threshold autoregressive (SETAR) model is used to model time series data, in order to allow for higher degree of flexibility in model parameters through a regime switching behaviour (Tong, 1990). Given a time-series data y_t, the SETAR model is used to predict future values, assuming that the behavior of the time series changes once the series enters a different regime. This switch from one to another regime depends on the past values of the series. The model consists of k autoregressive (AR) parts, each for a different regime. The model is usually denoted as SETAR (k, p) where k is the number of threshold, there are $k + 1$ number of regime in the model and p is the order of the autoregressive part. For example, suppose an AR(1) model is assumed in both regimes, then a 2-regime SETAR model is given by Franses et al

(2000):

$$\begin{aligned} y_t &= \phi_{0,1} + \phi_{1,1} y_{t\ \ 1} + \epsilon_t \ \text{ if } \ y_{t\ \ 1} \quad c, \\ &= \phi_{0,2} + \phi_{1,2} y_{t\ \ 1} + \epsilon_t \ \text{ if } \ y_{t\ \ 1} > c, \end{aligned} \tag{7}$$

where for the moment the ϵ_t are assumed to be an i.i.d. white noise sequence conditional upon the history of the time series and c is the threshold value. The SETAR model assumes that the border between the two regimes is given by a specific value of the threshold variable $y_{t\ \ 1}$. The model can be implemented using 'setar' function under the "tsDyn" package in R (Di Narzo et al, 2020).

4.6 Bayesian structural time series (BSTS) model

Bayesian Statistics has many applications in the field of statistical techniques such as regression, classification, clustering, and time series analysis. Scott and Varian (Scott and Varian, 2014) used structural time series models to show how Google search data can be used to improve short-term forecasts of economic time series. In the structural time series model, the observation in time t, y_t is defined as follows:

$$y_t = X_t^T \beta_t + \epsilon_t \tag{8}$$

where β_t is the vector of latent variables, X_t is the vector of model parameters, and ϵ_t are assumed follow Normal distributions with zero mean and H_t as the variance. In addition, β_t is represented as follows:

$$\beta_{t+1} = S_t \beta_t + R_t \delta_t, \tag{9}$$

where δ_t are assumed to follow Normal distributions with zero mean and Q_t as the variance. Gaussian distribution is selected as the prior of the BSTS model since we use the occurred frequency values ranging from 0 to 1 (Jammalamadaka et al, 2018). An R implementation is available under the "bsts" package (Scott et al, 2020), where one can add local linear trend and seasonal components as required. The state specification is passed as an argument to 'bsts' function, along with the data and the desired number of Markov chain Monte Carlo (MCMC) iterations, and the model is fit using an MCMC algorithm (Scott and Varian, 2013).

4.7 Theta model

The 'Theta method' or 'Theta model' is a univariate time series forecasting technique that performed particularly well in M3 forecasting competition and of interest to forecasters (Assimakopoulos and Nikolopoulos, 2000). The method decomposes the original data into two or more lines, called theta lines, and extrapolates them using forecasting models. Finally, the predictions are combined to obtain the final forecasts. The theta lines can be estimated by simply modifying the 'curvatures' of the original time series (Spiliotis et al, 2020). This change is obtained from a coefficient, called θ coefficient, which is directly applied to the second differences of the time series:

$$Y^{"}_{new}(\theta) = \theta Y^{"}_{data}, \tag{10}$$

where $Y^{"}_{data} = Y_t \quad 2Y_{t\ \ 1} + Y_{t\ \ 2}$ at time t for $t = 3, 4, \quad , n$ and $\{Y_1, Y_2, \quad , Y_n\}$ denote the observed univariate time series. In practice, coefficient θ can be considered as a transformation parameter which creates a series of the same mean and slope with that of the

original data but having different variances. Now, Eqn. (10) is a second-order difference equation and has solution of the following form (Hyndman and Billah, 2003):

$$Y_{new}(\theta) = a_\theta + b_\theta(t \quad 1) + \theta Y_t, \tag{11}$$

where a_θ and b_θ are constants and $t = 1, 2, \quad , n$. Thus, $Y_{new}(\theta)$ is equivalent to a linear function of Y_t with a linear trend added. The values of a_θ and b_θ are computed by minimizing the sum of squared differences:

$$\sum_{i=1}^{t} [Y_t \quad Y_{new}(\theta)]^2 = \sum_{i=1}^{t} [(1 \quad \theta)Y_t \quad a_\theta \quad b_\theta(t \quad 1)]^2 . \tag{12}$$

Forecasts from the Theta model are obtained by a weighted average of forecasts of $Y_{new}(\theta)$ for different values of θ. Also, the prediction intervals and likelihood-based estimation of the parameters can be obtained based on a state-space model, demonstrated in Hyndman and Billah (2003). An R implementation of the Theta model is possible with 'thetaf' function in "forecast" package (Hyndman et al, 2020).

4.8 TBATS model

The main objective of TBATS model is to deal with complex seasonal patterns using exponential smoothing (De Livera et al, 2011). The name is acronyms for key features of the models: Trigonometric seasonality (T), Box-Cox Transformation (B), ARMA errors (A), Trend (T) and Seasonal (S) components. TBATS makes it easy for users to handle data with multiple seasonal patterns. This model is preferable when the seasonality changes over time (Hyndman and Athanasopoulos, 2018). TBATS models can be described as follows:

$$\begin{aligned} y_t^{(\mu)} &= l_t \ _1 + \phi b_t \ _1 + \sum_{i=1}^{T} s_t^{(i)} \ _{m_i} + d_t \\ l_t &= l_t \ _1 + \phi b_t \ _1 + \alpha d_t \\ b_t &= \phi b_t \ _1 + \beta d_t \\ d_t &= \sum_{i=1}^{p} \psi_i d_t \ _i + \sum_{j=1}^{q} \theta_j e_t \ _j + e_t; \end{aligned} \tag{13}$$

where $y_t^{(\mu)}$ is the time series at time point t (Box-Cox Transformed), $s_t^{(i)}$ is the i-th seasonal component, l_t is the local level, b_t is the trend with damping, d_t is the ARMA(p, q) process for residuals and e_t as the Gaussian white noise. TBATS model can be implemented using 'tbats' function under the "forecast" package in R statistical software (Hyndman et al, 2020).

4.9 Artificial neural networks (ANN) model

Forecasting with artificial neural networks (ANN) has received increasing interest in various research and applied domains in the late 1990s. It has been given special attention in epidemiological forecasting (Philemon et al, 2019). Multi-layered feed-forward neural networks with back-propagation learning rules are the most widely used models with applications in classification and prediction problems (Zhang et al, 1998). There is a single

hidden layer between the input and output layers in a simple feed-forward neural net, and where weights connect the layers. Denoting by ω_{ji} the weights between the input layer and hidden layer and ν_{kj} denotes the weights between the hidden and output layers. Based on the given inputs x_i, the neuron's net input is calculated as the weighted sum of its inputs. The output layer of the neuron, y_j, is based on a sigmoidal function indicating the magnitude of this net-input (Goodfellow et al, 2016). For the j^{th} hidden neuron, the calculation for the net input and output are:

$$net_j^h = \sum_{i=1}^{n} \omega_{ji} x_i \tag{14}$$

$$y_j = f(net_j^h). \tag{15}$$

For the k^{th} output neuron:

$$net_k^o = \sum_{j=1}^{J+1} \nu_{kj} y_j \tag{16}$$

$$o_k = f(net_k^o), \tag{17}$$

where $f(net) = \frac{1}{1+e^{-\lambda net}}$ with λ 2 $(0, 1)$ is a parameter used to control the gradient of the function and J is the number of neurons in the hidden layer. The back-propagation (Rumelhart et al, 1985) learning algorithm is the most commonly used technique in ANN. In the error back-propagation step, the weights in ANN are updated by minimizing

$$E = \frac{1}{2P} \sum_{p=1}^{P} \sum_{k=1}^{K} (d_{pk} \quad O_{pk})^2, \tag{18}$$

where, d_{pk} is the desired output of neuron k and for input pattern p. The common formula for number of neurons in the hidden layer is $h = \frac{(i+j)}{2} + \sqrt{p}\overline{d}$, for selecting the number of hidden neurons, where i is the number of output y_j and d denotes the number of i training patterns in the input x_i (Zhang and Qi, 2005). The application of ANN for time series data is possible with 'mlp' function under "nnfor" package in R (Kourentzes, 2017b).

4.10 Autoregressive neural network (ARNN) model

Autoregressive neural network (ARNN) received attention in time series literature in late 1990s (Faraway and Chatfield, 1998). The architecture of a simple feedforward neural network can be described as a network of neurons arranged in input layer, hidden layer, and output layer in a prescribed order. Each layer passes the information to the next layer using weights that are obtained using a learning algorithm (Zhang and Qi, 2005). ARNN model is a modification to the simple ANN model especially designed for prediction problems of time series datasets (Faraway and Chatfield, 1998). ARNN model uses a pre-specified number of lagged values of the time series as inputs and number of hidden neurons in its architecture is also fixed (Hyndman and Athanasopoulos, 2018). ARNN(p, k) model uses p lagged inputs of the time series data in a one hidden layered feedforward neural network with k hidden units in the hidden layer. Let $\underline{x}$ denotes a p-lagged inputs and f is a neural network of the following architecture:

$$f(\underline{x}) = c_0 + \sum_{j=1}^{k} w_j \phi \left(a_j + b_j^{\emptyset} \underline{x} \right); \tag{19}$$

where c_0, a_j, w_j are connecting weights, b_j are p-dimensional weight vector and ϕ is a bounded nonlinear sigmoidal function (e.g., logistic squasher function or tangent hyperbolic activation function). These Weights are trained using a gradient descent backpropagation (Rumelhart et al, 1985). Standard ANN faces the dilemma to choose the number of hidden neurons in the hidden layer and optimal choice is unknown. But for ARNN model, we adopt the formula $k = [(p + 1)/2]$ for non-seasonal time series data where p is the number of lagged inputs in an autoregressive model (Hyndman and Athanasopoulos, 2018). ARNN model can be applied using the 'nnetar' function available in the R statistical package "forecast" (Hyndman et al, 2020).

4.11 Ensemble forecasting models

The idea of ensemble time series forecasts was given by Bates and Granger (1969) in their seminal work (Bates and Granger, 1969). Forecasts generated from ARIMA, ETS, Theta, ARNN, WARIMA can be combined with equal weights, weights based on in-sample errors, or cross-validated weights. In the ensemble framework, cross-validation for time series data with user-supplied models and forecasting functions is also possible to evaluate model accuracy (Shaub, 2020). Combining several candidate models can hedge against an incorrect model specification. Bates and Granger(1969) (Bates and Granger, 1969) suggested such an approach and observed, somewhat surprisingly, that the combined forecast can even outperform the single best component forecast. While combination weights selected equally or proportionally to past model errors are possible approaches, many more sophisticated combination schemes, have been suggested. For example, rather than normalizing weights to sum to unity, unconstrained and even negative weights could be possible (Granger and Ramanathan, 1984). The simple equal-weights combination might appear woefully obsolete and probably non-competitive compared to the multitude of sophisticated combination approaches or advanced machine learning and neural network forecasting models, especially in the age of big data. However, such simple combinations can still be competitive, particularly for pandemic time series (Shaub, 2020). A flow diagram of the ensemble method is presented in Figure 2.

The ensemble method by Bates and Granger (1969) produces forecasts out to a horizon h by applying a weight w_m to each m of the n model forecasts in the ensemble. The ensemble forecast $f(i)$ for time horizon 1 i h and with individual component model forecasts $f_m(i)$ is then

$$f(i) = \sum_{m=1}^{n} w_m f_m(i). \tag{20}$$

The weights can be determined in several ways (for example, supplied by the user, set equally, determined by in-sample errors, or determined by cross-validation). The "forecastHybrid" package in R includes these component models in order to enhance the "forecast" package base models with easy ensembling (e.g., 'hybridModel' function in R statistical software) (Shaub and Ellis, 2019).

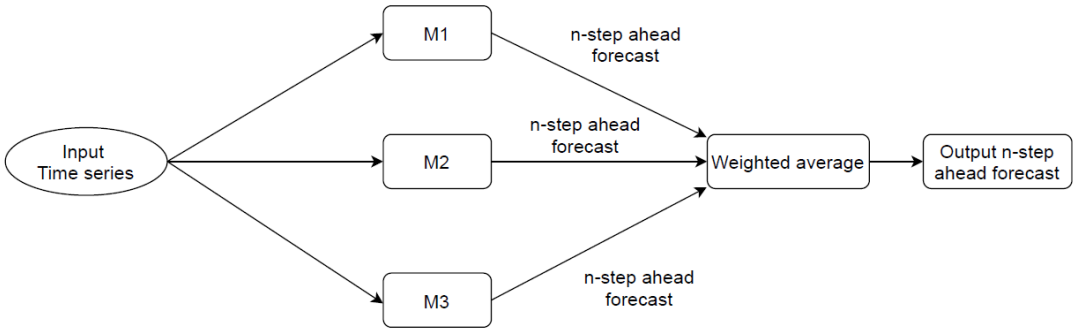

Fig. 2 Flow diagram of the ensemble model where M1, M2, and M3 are three different univariate time series models

4.12 Hybrid forecasting models

The idea of hybridizing time series models and combining different forecasts was first introduced by Zhang (2003) and further extended by Khashei and Bijari (2010); Chakraborty et al (2019); Chakraborty and Ghosh (2020); Chakraborty et al (2020). The hybrid forecasting models are based on an error re-modeling approach, and there are broadly two types of error calculations popular in the literature, which are given below (Mosleh and Apostolakis, 1986):

Definition 1 In the additive error model, the forecaster treats the expert's estimate as a variable, $\hat{Y}_t$, and thinks of it as the sum of two terms:

$$\hat{Y}_t = Y_t + e_t, \tag{21}$$

where Y_t is the true value and e_t be the additive error term.

Definition 2 In the multiplicative error model, the forecaster treats the expert's estimate $\hat{Y}_t$ as the product of two terms:

$$\hat{Y}_t = Y_t \quad e_t, \tag{22}$$

where Y_t is the true value and e_t be the multiplicative error term.

Now, even if the relationship is of product type, in the log-log scale it becomes additive. Hence, without loss of generality, we may assume the relationship to be additive and expect errors (additive) of a forecasting model to be random shocks (Chakraborty et al, 2020). These hybrid models are useful for complex correlation structures where less amount of knowledge is available about the data generating process. A simple example is the daily confirmed cases of the COVID-19 cases for various countries where very little is known about the structural properties of the current pandemic. The mathematical formulation of the proposed hybrid model (Z_t) is as follows:

$$Z_t = L_t + N_t, \tag{23}$$

where L_t is the linear part and N_t is the nonlinear part of the hybrid model. We can estimate both L_t and N_t from the available time series data. Let $\hat{L}_t$ be the forecast value

of the linear model (e.g., ARIMA) at time t and ϵ_t represent the error residuals at time t, obtained from the linear model. Then, we write

$$\epsilon_t = Z_t \quad \hat{L}_t. \tag{24}$$

These left-out residuals are further modeled by a nonlinear model (e.g., ANN or ARNN) and can be represented as follows:

$$\epsilon_t = f(\epsilon_{t\ 1}, \epsilon_{t\ 2}, ..., \epsilon_{t\ p}) + \varepsilon_t, \tag{25}$$

where f is a nonlinear function, and the modeling is done by the nonlinear ANN or ARNN model as defined in Eqn. (19) and ε_t is supposed to be the random shocks. Therefore, the combined forecast can be obtained as follows:

$$\hat{Z}_t = \hat{L}_t + \hat{N}_t, \tag{26}$$

where $\hat{N}_t$ is the forecasted value of the nonlinear time series model. An overall flow diagram of the proposed hybrid model is given in Figure 3. In the hybrid model, a nonlinear model is applied in the second stage to re-model the left-over autocorrelations in the residuals, which the linear model could not model. Thus, this can be considered as an error re-modeling approach. This is important because due to model misspecification and disturbances in the pandemic rate time series, the linear models may fail to generate white noise behavior for the forecast residuals. Thus, hybrid approaches eventually can improve the predictions for the epidemiological forecasting problems, as shown in Chakraborty et al (2019); Chakraborty and Ghosh (2020); Chakraborty et al (2020). These hybrid models only assume that the linear and nonlinear components of the epidemic time series can be separated individually. The implementation of the hybrid models used in this study are available in https://github.com/indrajitg-r/COVID.

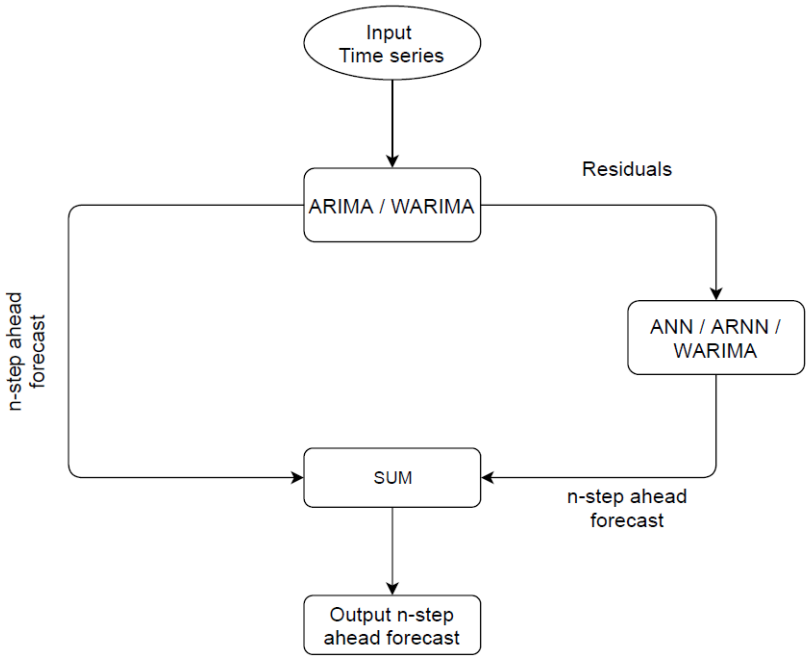

Fig. 3 Flow diagram of the hybrid forecasting model

Table 2 Description of COVID-19 datasets

Countries	Start date	End date	Length
USA	20/01/2020	15/09/2020	240
India	29/01/2020	15/09/2020	231
Brazil	25/02/2020	15/09/2020	204
Russia	31/01/2020	15/09/2020	229
Peru	06/03/2020	15/09/2020	194

5 Experimental analysis

Five time series COVID-19 datasets for the USA, India, Russia, Brazil, and Peru UK are considered for assessing twenty forecasting models (individual, ensemble, and hybrid). The datasets are mostly nonlinear, nonstationary, and non-gaussian in nature. We have used root mean square error (RMSE), mean absolute error (MAE), mean absolute percentage error (MAPE), and symmetric MAPE (SMAPE) to evaluate the predictive performance of the models used in this study. Since the number of data points in both the datasets is limited, advanced deep learning techniques will over-fit the datasets (Hastie et al, 2009).

5.1 Datasets

We use publicly available datasets to compare various forecasting frameworks. COVID-19 cases of five countries with the highest number of cases were collected from https://www.worldometers.info/ and https://ourworldindata.org/. The datasets and their description is presented in Table 2.

5.2 Global characteristics

Characteristics of these five time series were examined using Hurst exponent, KPSS test and Terasvirta test and other measures as described in 3. Hurst exponent (denoted by H), which ranges between zero to one, is calculated to measure the long-range dependency in a time series and provides a measure of long-term nonlinearity. For values of H near zero, the time series under consideration is mean-reverting. An increase in the value will be followed by a decrease in the series and vice versa. When H is close to 0.5, the series has no autocorrelation with past values. These types of series are often called Brownian motion. When H is near one, an increase or decrease in the value is most likely to be followed by a similar movement in the future. All the five COVID-19 datasets in this study possess the Hurst exponent value near one, which indicates that these time series datasets have a strong trend of increase followed by an increase or decrease followed by another decline.

KPSS tests are performed to examine the stationarity of a given time series. The null hypothesis for the KPSS test is that the time series is stationary. Thus, the series is nonstationary when the p-value less than a threshold. From Table 3, all the five datasets can be characterized as non-stationary as the p-value < 0.01 in each instances. Terasvirta test examines the linearity of a time series against the alternative that a nonlinear process has generated the series. It is observed that the USA, India, Russia, and Brazil COVID-19 datasets are likely to follow a nonlinear trend. On the other hand, Peru data shows some linear trend.

Further, we examine serial correlation, skewness, kurtosis, and maximum Lyapunov exponent for the five COVID-19 datasets. The results are reported in Table 4. The serial

Table 3 Test results on COVID-19 datasets

Countries	**Hurst exponent**	**KPSS test**	**Terasvirta test**
USA	0.9996	p-value < 0.01	p-value $= 0.01$
India	0.9997	p-value < 0.01	p-value < 0.01
Brazil	0.9974	p-value < 0.01	p-value < 0.01
Russia	0.9992	p-value < 0.01	p-value $= 0.05$
Peru	0.9983	p-value < 0.01	p-value $= 0.84$

Table 4 Characteristics of COVID-19 datasets

Countries	**Box test**	**Skewness**	**Kurtosis**	**Chaotic/Non-chaotic**
USA	p-value < 0.01	0.4971	- 0.7465	Non-chaotic
India	p-value < 0.01	1.4981	0.9422	Non-chaotic
Brazil	p-value < 0.01	0.6897	-0.7124	Non-chaotic
Russia	p-value < 0.01	- 0.0544	-1.4439	Non-chaotic
Peru	p-value < 0.01	0.4421	-0.2142	Non-chaotic

Table 5 R functions and packages for implementation.

Model	R function	R package	Reference
ARIMA	auto.arima	forecast	Hyndman et al (2007)
ETS	ets	forecast	Hyndman et al (2007)
SETAR	setar	tsDyn	Di Narzo et al (2020)
TBATS	tbats	forecast	Hyndman et al (2007)
Theta	thetaf	forecast	Hyndman et al (2007)
ANN	mlp	nnfor	Kourentzes (2017a)
ARNN	nnetar	forecast	Hyndman et al (2007)
WARIMA	WaveletFittingarma	WaveletArima	Paul et al (2017)
BSTS	bsts	bsts	Scott et al (2020)
ARFIMA	arfima	forecast	Hyndman et al (2007)
Ensemble models	hybridModel	forecastHybrid	Shaub and Ellis (2019)
Hybrid models	-	-	https://github.com/indrajitg-r/COVID

correlation of the datasets is computed using the Box-Pierce test statistic for the null hypothesis of independence in a given time series. The p-values related to each of the datasets were found to be below the significant level (see Table 4). This indicates that these COVID-19 datasets have no serial correlation when lag equals one. Skewness for Russia COVID-19 dataset is found to be negative, whereas the other four datasets are positively skewed. This means for the Russia dataset; the left tail is heavier than the right tail. For the other four datasets, the right tail is heavier than the left tail. The Kurtosis values for the India dataset are found positive while the other four datasets have negative kurtosis values. Therefore, the COVID-19 dataset of India tends to have a peaked distribution, and the other four datasets may have a flat distribution. We observe that each of the five datasets is non-chaotic in nature, i.e., the maximum Lyapunov exponents are less than unity. A summary of the implementation tools is presented in Table 5.

Table 6 Pandemic datasets and corresponding ACF, PACF plots with 15-days test data

Country	Data	ACF plot	PACF plot
USA	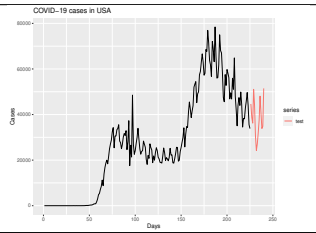	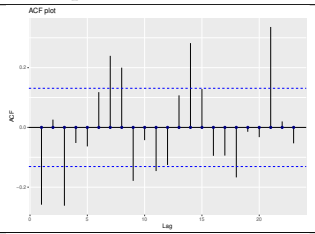	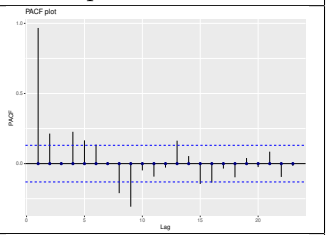
India	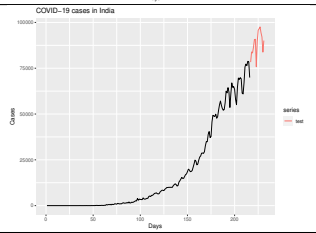	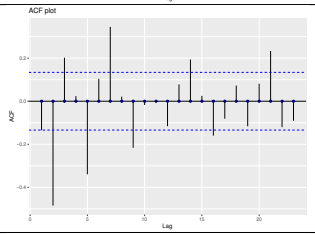	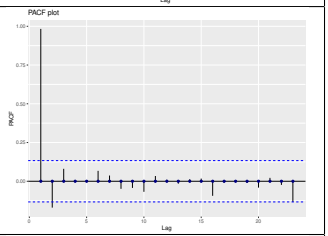
Brazil	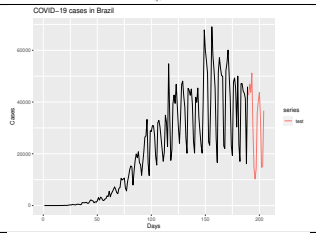	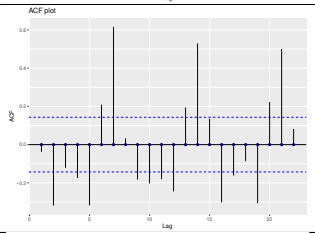	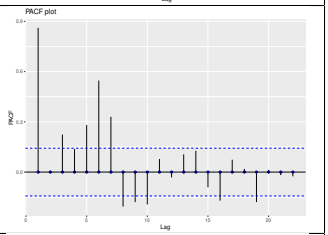
Russia	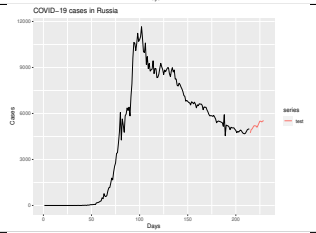	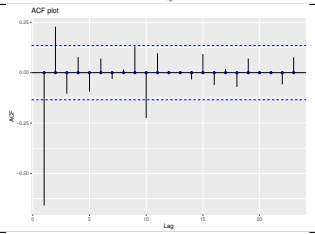	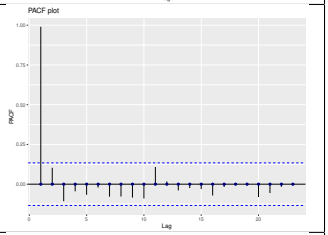
Peru	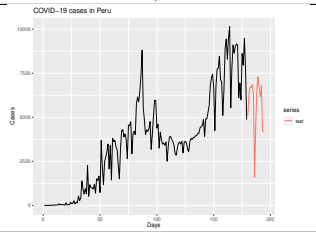	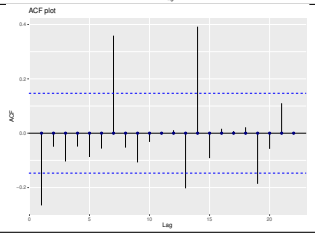	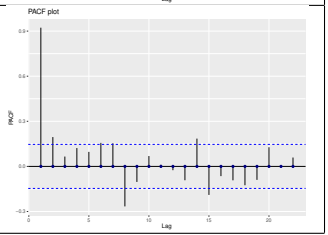

5.3 Accuracy metrics

We used four popular accuracy metrics to evaluate the performance of different time series forecasting models. The expressions of these metrics are given below.

$$RMSE = \sqrt{\frac{1}{n}\sum_{i=1}^{n}(y_i \quad \hat{y}_i)^2};\ MAE = \frac{1}{n}\sum_{i=1}^{n} j y_i \quad \hat{y}_i j; \tag{27}$$

$$MAPE = \frac{1}{n}\sum_{i=1}^{n} j\frac{\hat{y}_i \quad y_i}{y_i} j \quad 100;\ SMAPE = \frac{1}{n}\sum_{i=1}^{n}\frac{j\hat{y}_i \quad y_i j}{(j\hat{y}_i j + j y_i j)/2} \quad 100;$$

where y_i are actual series values, $\hat{y}_i$ are the predictions by different models and n represent the number of data points of the time series. The models with least accuracy metrics is the best forecasting model.

Table 7 Pandemic datasets and corresponding ACF, PACF plots with 30-days test data

Country	Data	ACF plot	PACF plot
USA	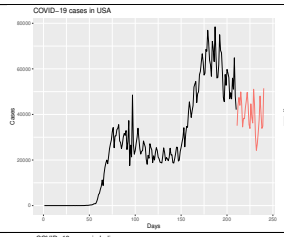	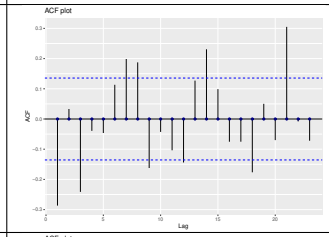	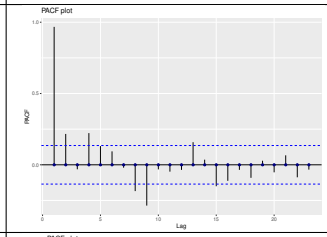
India	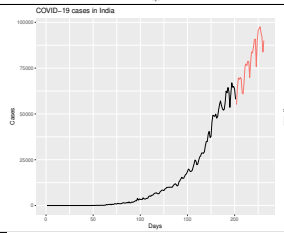	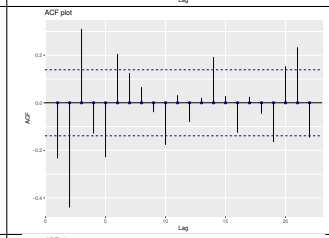	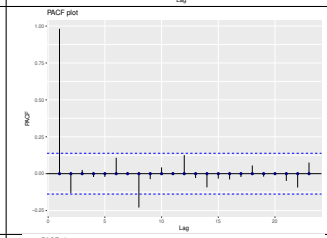
Brazil	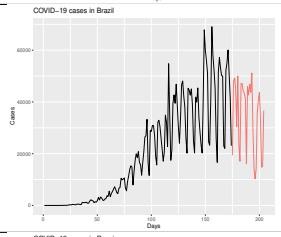	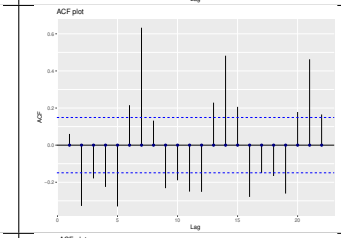	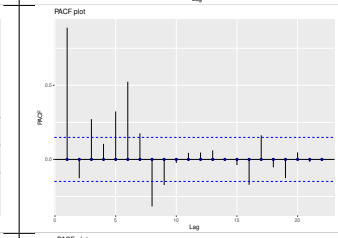
Russia	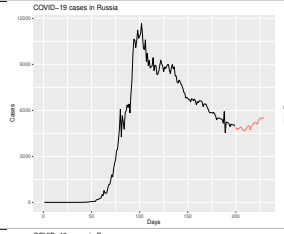	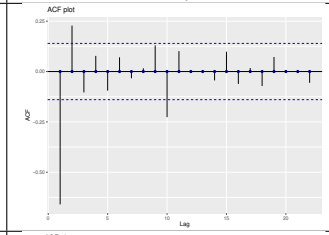	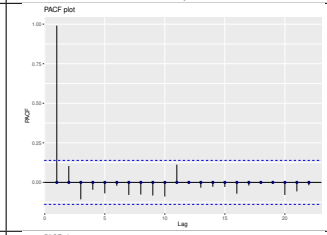
Peru	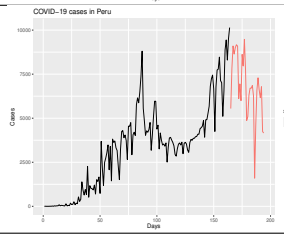	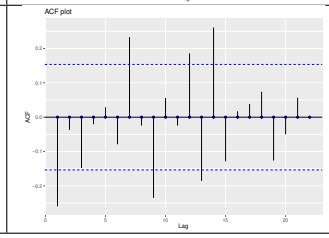	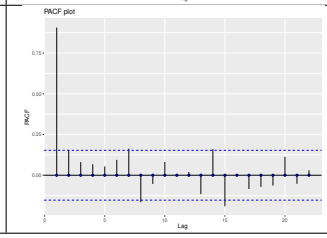

5.4 Analysis of results

This subsection is devoted to the experimental analysis of confirmed COVID-19 cases using different time series forecasting models. The test period is chosen to be 15 days and 30 days, whereas the rest of the data is used as training data (see Table 2). In first columns of Tables 6 and 7, we present training data and test data for USA, India, Brazil, Russia and Peru. The autocorrelation function (ACF) and partial autocorrelation function (PACF) plots are also depicted for the training period of each of the five countries in Tables 6 and 7.

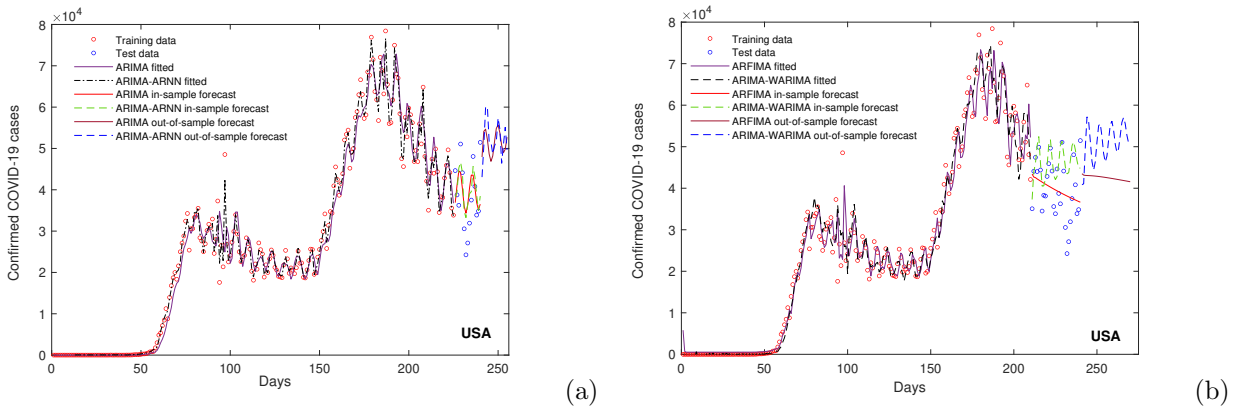

Fig. 4 Plots of (a) 15-days ahead forecast results for USA COVID-19 data obtained using ARIMA and hybrid ARIMA-ARNN models. (b) 30-days ahead forecast results from ARFIMA and hybrid ARIMA-WARIMA models.

ACF and PACF plots are generated after applying the required number of differencing of each training data using the r function 'diff'. The required order of differencing is obtained by using the R function 'ndiffs' which estimate the number of differences required to make a given time series stationary. The integer-valued order of differencing is then used as the value of 'd' in the ARIMA(p, d, q) model. Other two parameters 'p' and 'q' of the model are obtained from ACF and PACF plots respectively (see Tables 6 and 7). However, we choose the 'best' fitted ARIMA model using AIC value for each training dataset. Table 6 presents the training data (black colored) and test data (red-colored) and corresponding ACF and PACF plots for the five time-series datasets.

Further, we checked twenty different forecasting models as competitors for the short-term forecasting of COVID-19 confirmed cases in five countries. 15-days and 30-days ahead forecasts were generated for each model, and accuracy metrics were computed to determine the best predictive models. From the ten popular single models, we choose the best one based on the accuracy metrics. On the other hand, one hybrid/ensemble model is selected from the rest of the ten models. The best-fitted ARIMA parameters, ETS, ARNN, and ARFIMA models for each country are reported in the respective tables. Table 7 presents the training data (black colored) and test data (red-colored) and corresponding plots for the five datasets. Twenty forecasting models are implemented on these pandemic time-series datasets. Table 5 gives the essential details about the functions and packages required for implementation.

5.4.1 Results for USA COVID-19 data

Among the single models, ARIMA(2,1,4) performs best in terms of accuracy metrics for 15-days ahead forecasts. TBATS and ARNN(16,8) also have competitive accuracy metrics. Hybrid ARIMA-ARNN model improves the earlier ARIMA forecasts and has the best accuracy among all hybrid/ensemble models (see Table 8). Hybrid ARIMA-WARIMA also does a good job and improves ARIMA model forecasts. In-sample and out-of-sample forecasts obtained from ARIMA and hybrid ARIMA-ARNN models are depicted in Fig. 4(a). Out-of-sample forecasts are generated using the whole dataset as training data.

ARFIMA(2,0,0) is found to have the best accuracy metrics for 30-days ahead forecasts among single forecasting models. BSTS and SETAR also have good agreement with the test data in terms of accuracy metrics. Hybrid ARIMA-WARIMA model and has the best

Table 8 Performance metrics with 15 days-ahead test set for USA

Model	15-days ahead forecast			
	RMSE	MAE	MAPE	SMAPE
ARIMA(2,1,4)	**7187.02**	**6094.95**	**16.89**	**16.07**
ETS(A,N,N)	8318.73	6759.65	17.82	17.86
SETAR	8203.21	6725.96	18.19	17.77
TBATS	7351.04	6367.46	17.86	16.73
Theta	8112.22	6791.52	18.51	17.95
ANN	9677.105	8386.223	25.15	21.69
ARNN(16,8)	7633.92	6647.18	19.75	17.42
WARIMA	9631.98	8182.84	21.09	22.21
BSTS	10666.15	8527.72	20.91	23.26
ARFIMA(1,0.14,1)	8413.33	6696.09	17.48	17.68
Hybrid ARIMA-ANN	7113.72	6058.29	16.90	15.99
Hybrid ARIMA-ARNN	**5978.04**	**4650.89**	**13.22**	**12.45**
Hybrid ARIMA-WARIMA	6582.93	5217.023	14.33	13.80
Hybrid WARIMA-ANN	10633.97	8729.11	21.85	24.22
Hybrid WARIMA-ARNN	9558.34	8138.71	21.05	22.05
Ensemble ARIMA-ETS-Theta	7602.06	6388.96	17.32	16.89
Ensemble ARIMA-ETS-ARNN	7012.95	6184.23	18.09	16.45
Ensemble ARIMA-Theta-ARNN	6933.88	6054.97	17.42	16.07
Ensemble ETS-Theta-ARNN	7044.20	5950.40	16.97	15.82
Ensemble ANN-ARNN-WARIMA	7437.21	6465.18	18.66	17.11

Table 9 Performance metrics with 30 days-ahead test set for USA

Model	30-days ahead forecast			
	RMSE	MAE	MAPE	SMAPE
ARIMA(2,1,4) with drift	12370.18	10499.44	29.87	24.26
ETS(A,Ad,N)	11929.897	9951.090	28.95	23.49
SETAR	8593.527	6904.605	20.18	17.25
TBATS	10314.23	8587.83	24.95	20.73
Theta	12234.16	9858.115	29.03	23.24
ANN	15241.65	12973.2	37.11	28.86
ARNN(16,8)	19000.09	17311.86	46.95	36.01
WARIMA	12455.31	9501.018	22.55	27.45
BSTS	8459.763	6444.994	15.94	16.87
ARFIMA(2,0,0)	**6847.32**	**5651.33**	**14.83**	**14.40**
Hybrid ARIMA-ANN	12269.99	10339.18	29.46	23.92
Hybrid ARIMA-ARNN	12584.03	10566.16	30.14	24.32
Hybrid ARIMA-WARIMA	**8514.36**	**6702.07**	**19.52**	**16.59**
Hybrid WARIMA-ANN	14983.09	11918.16	28.55	36.52
Hybrid WARIMA-ARNN	12294.48	9330.15	22.14	26.88
Ensemble ARIMA-ETS-Theta	12014.39	9978.22	29.04	23.49
Ensemble ARIMA-ETS-ARNN	11484.49	10035.78	28.35	23.49
Ensemble ARIMA-Theta-ARNN	13596.9	12000.69	33.86	27.21
Ensemble ETS-Theta-ARNN	13074.13	11429.5	32.52	26.26
Ensemble ANN-ARNN-WARIMA	11652.2	9947.16	30.60	24.23

Table 10 Performance metrics with 15 days-ahead test set for India

Model	15-days ahead forecast			
	RMSE	MAE	MAPE	SMAPE
ARIMA(1,2,5)	8141.76	7479.43	8.36	8.72
ETS(A,A,N)	15431	14415.73	15.92	17.18
SETAR	22835.95	21851.45	24.24	27.84
TBATS	11764.61	10837.68	12.00	12.89
Theta	18405.29	17403.03	19.24	21.50
ANN	**6663.10**	**5891.94**	**6.54**	**6.81**
ARNN(2,2)	25617.9	24539.67	27.23	31.86
WARIMA	12201.48	11103.41	12.25	13.18
BSTS	13535.1	12402.34	13.65	14.84
ARFIMA(0,0.49,4)	34848.86	33323.88	37.03	46.25
Hybrid ARIMA-ANN	8080.862	7399.7	8.28	8.64
Hybrid ARIMA-ARNN	**7762.32**	**6560.26**	**7.20**	**7.67**
Hybrid ARIMA-WARIMA	8144.77	7455.34	8.32	8.68
Hybrid WARIMA-ANN	11883.45	10697.21	11.79	12.65
Hybrid WARIMA-ARNN	11623.15	10339.16	11.33	12.17
Ensemble ARIMA-ETS-Theta	13734.28	12641.35	13.93	15.14
Ensemble ARIMA-ETS-ARNN	15940.9	14941.65	16.50	18.17
Ensemble ARIMA-Theta-ARNN	16883.48	15897.06	17.57	19.45
Ensemble ETS-Theta-ARNN	19750.31	18780.61	20.79	23.42
Ensemble ANN-ARNN-WARIMA	14512.1	13496.63	14.88	16.25

accuracy among all hybrid/ensemble models (see Table 9). In-sample and out-of-sample forecasts obtained from ARFIMA and hybrid ARIMA-WARIMA models are depicted in Fig. 4(b).

5.4.2 Results for India COVID-19 data

Among the single models, ANN performs best in terms of accuracy metrics for 15-days ahead forecasts. ARIMA(1,2,5) also has competitive accuracy metrics in the test period. Hybrid ARIMA-ARNN model improves the ARIMA(1,2,5) forecasts and has the best accuracy among all hybrid/ensemble models (see Table 10). Hybrid ARIMA-ANN and hybrid ARIMA-WARIMA also do a good job and improves ARIMA model forecasts. In-sample and out-of-sample forecasts obtained from ANN and hybrid ARIMA-ARNN models are depicted in Fig. 5(a). Out-of-sample forecasts are generated using the whole dataset as training data (see Fig. 5).

ANN is found to have the best accuracy metrics for 30-days ahead forecasts among single forecasting models for India COVID-19 data. Ensemble ANN-ARNN-WARIMA model and has the best accuracy among all hybrid/ensemble models (see Table 11). In-sample and out-of-sample forecasts obtained from ANN and ensemble ANN-ARNN-WARIMA models are depicted in Fig. 5(b).

5.4.3 Results for Brazil COVID-19 data

Among the single models, SETAR performs best in terms of accuracy metrics for 15-days ahead forecasts. Ensemble ETS-Theta-ARNN (EFN) model has the best accuracy among all hybrid/ensemble models (see Table 12). In-sample and out-of-sample forecasts obtained from SETAR and ensemble EFN models are depicted in Fig. 6(a).

Table 11 Performance metrics with 30 days-ahead test set for India

Model	30-days ahead forecast			
	RMSE	MAE	MAPE	SMAPE
ARIMA(1,2,5)	17755.52	15657.27	18.67	21.01
ETS(A,A,N)	14873.78	13051.98	15.57	17.18
SETAR	21527.58	18609.71	21.98	25.49
TBATS	24849.07	21843.15	25.96	30.82
Theta	21713.03	19191.21	22.84	26.47
ANN	**6379.91**	**4800.13**	**6.48**	**6.13**
ARNN(8,4)	13225.43	10287.29	11.90	13.06
WARIMA	14720.81	12738.66	15.15	16.72
BSTS	14332.3	12493.74	14.88	16.34
ARFIMA(0,0.5,4)	40115.62	36452.33	43.87	58.73
Hybrid ARIMA-ANN	17640.51	15535.58	18.53	20.83
Hybrid ARIMA-ARNN	17580.41	15507.04	18.51	20.80
Hybrid ARIMA-WARIMA	17869.14	15771.05	18.78	21.19
Hybrid WARIMA-ANN	14616.89	12613.57	15	16.53
Hybrid WARIMA-ARNN	16052.8	14067.29	16.83	18.74
Ensemble ARIMA-ETS-Theta	18081.97	15928.84	18.96	21.40
Ensemble ARIMA-ETS-ARNN	15615.2	13419.82	15.86	17.61
Ensemble ARIMA-Theta-ARNN	17933.14	15330.84	18.07	20.41
Ensemble ETS-Theta-ARNN	16442.65	14160.56	16.74	18.69
Ensemble ANN-ARNN-WARIMA	**9090.214**	**7427.787**	**8.83**	**9.32**

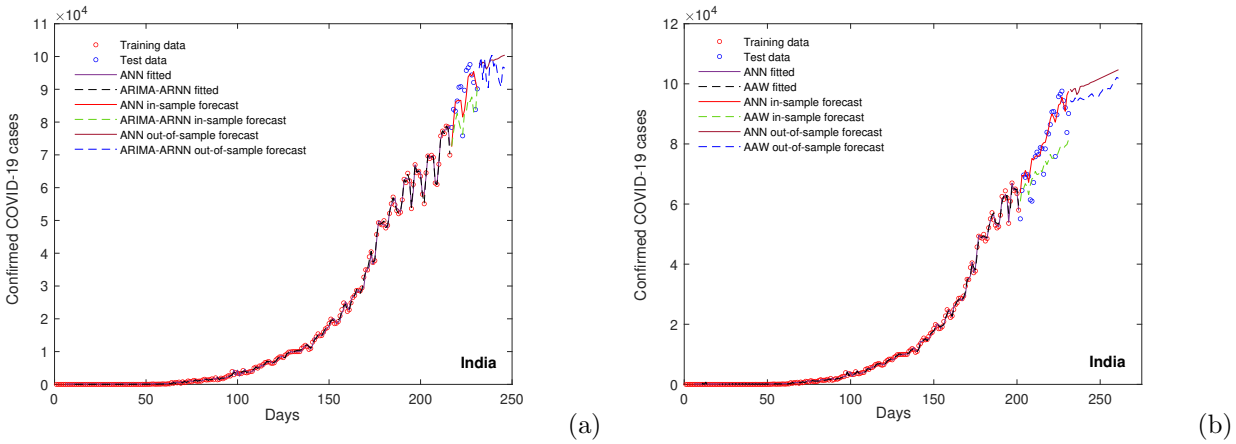

Fig. 5 Plots of (a) 15-days ahead forecast results for India COVID-19 data obtained using ANN and hybrid ARIMA-ARNN models and (b) 30-days ahead forecast results from ANN and ANN-ARNN-WARIMA (AAW) models.

WARIMA is found to have the best accuracy metrics for 30-days ahead forecasts among single forecasting models for Brazil COVID-19 data. Hybrid WARIMA-ANN model has the best accuracy among all hybrid/ensemble models (see Table 13). In-sample and out-of-sample forecasts obtained from WARIMA and hybrid WARIMA-ANN models are depicted in Fig. 6(b).

5.4.4 Results for Russia COVID-19 data

BSTS performs best in terms of accuracy metrics for a 15-days ahead forecast in the case of Russia COVID-19 data among single models. Theta and ARNN(3,2) also show competi-

Table 12 Performance metrics with 15 days-ahead test set for Brazil

Model	15-days ahead forecast			
	RMSE	MAE	MAPE	SMAPE
ARIMA(3,1,2)	16553.75	12530.04	76.62	41.66
ETS(A,A,N)	13793.618	11038.765	63.41	38.99
SETAR	**11645.6**	**10148.91**	**49.77**	**37.35**
TBATS	15842.01	11803.72	72.67	40.05
Theta	16263.93	12614.74	65.71	42.21
ANN	19622.3	16536.91	83.45	53.78
ARNN((19,10))	13733.19	11951.27	57.59	40.36
WARIMA	17167.66	13487.76	80.45	43.85
BSTS	21154.89	16702.38	98.97	49.62
ARFIMA(2,0.5,1)	14023.22	11109.03	63.94	39.03
Hybrid ARIMA-ANN	17541.86	13436.8	81.47	42.93
Hybrid ARIMA-ARNN	18151.56	15254.77	79.64	46.73
Hybrid ARIMA-WARIMA	16596.75	12704.16	77.16	41.94
Hybrid WARIMA-ANN	16797.05	13378.25	78.94	43.96
Hybrid WARIMA-ARNN	19211.01	16043.31	83.34	48.11
Ensemble ARIMA-ETS-Theta	15271.82	11497.86	70.54	39.68
Ensemble ARIMA-ETS-ARNN	13517.19	11260.21	62.81	39.61
Ensemble ARIMA-Theta-ARNN	14546.36	11975.91	66.79	41.13
Ensemble ETS-Theta-ARNN	**13431.11**	**11324.4**	**62.67**	**39.83**
Ensemble ANN-ARNN-WARIMA	15565.1	13201.37	71.83	44.10

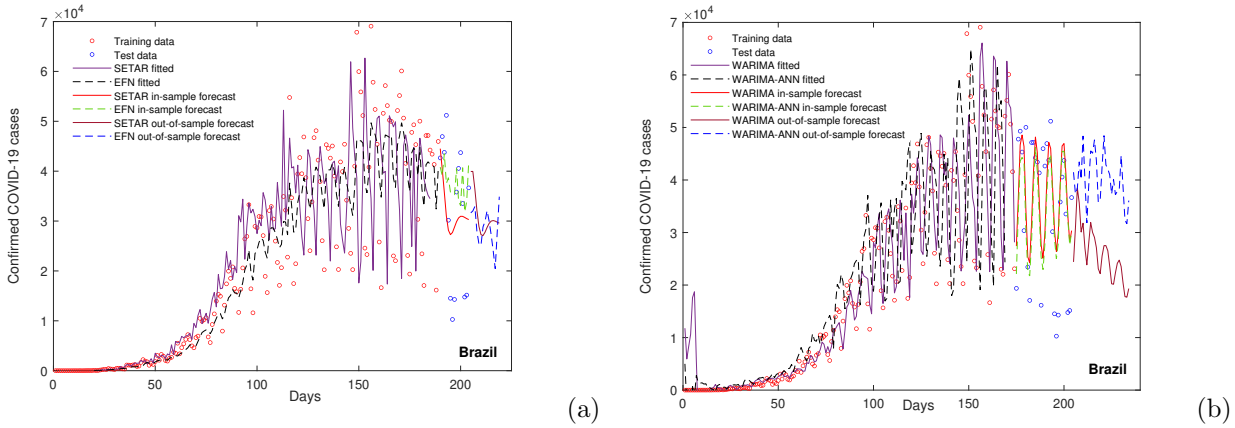

Fig. 6 Plots of (a) 15-days ahead forecast results for Brazil COVID-19 data obtained using SETAR and ETS-Theta-ARNN (EFN) models and (b) 30-days ahead forecast results from WARIMA and hybrid WARIMA-ANN models.

tive accuracy measures. Ensemble ETS-Theta-ARNN (EFN) model has the best accuracy among all hybrid/ensemble models (see Table 14). Ensemble ARIMA-ETS-ARNN and ensemble ARIMA-Theta-ARNN also performs well in the test period. In-sample and out-of-sample forecasts obtained from BSTS and ensemble EFN models are depicted in Fig. 7(a).

SETAR is found to have the best accuracy metrics for 30-days ahead forecasts among single forecasting models for Russia COVID-19 data. Ensemble ARIMA-Theta-ARNN (AFN) model has the best accuracy among all hybrid/ensemble models (see Table 15). All five ensemble models show promising results for this dataset. In-sample and out-of-sample forecasts obtained from SETAR and ensemble AFN models are depicted in Fig. 7(b).

Table 13 Performance metrics with 30 days-ahead test set for Brazil

Model	30-days ahead forecast			
	RMSE	MAE	MAPE	SMAPE
ARIMA(5,1,1) with drift	17647.13	14924.74	69.57	41.85
ETS(A,A,N)	20270.82	15186.14	81.30	42.45
SETAR	16136.69	15085.91	52.75	49.03
TBATS	14166.74	10629.13	56.19	33.78
Theta	17662.39	12880.03	70.55	38.38
ANN	22403	18241.79	90.86	47.29
ARNN(9,5)	13458.51	10884.02	40.10	30.92
WARIMA	**10628.51**	**9075.32**	**38.24**	**30.41**
BSTS	16876.78	15314.18	45.58	50.17
ARFIMA(2,0.5,1)	12647.79	11616.15	47.49	37.56
Hybrid ARIMA-ANN	17559.43	14810.82	69.11	41.58
Hybrid ARIMA-ARNN	17274.78	14511.77	67.87	41.00
Hybrid ARIMA-WARIMA	17464.81	14724.52	68.89	41.49
Hybrid WARIMA-ANN	**10841.65**	**8886.71**	**35.56**	**29.76**
Hybrid WARIMA-ARNN	10649.35	9104.54	38.39	30.48
Ensemble ARIMA-ETS-Theta	18096.57	13854.34	72.82	40.27
Ensemble ARIMA-ETS-ARNN	16186	13705.63	64.26	39.84
Ensemble ARIMA-Theta-ARNN	15406.54	12793.94	60.87	38.06
Ensemble ETS-Theta-ARNN	15737.01	12512.65	63.26	37.89
Ensemble ANN-ARNN-WARIMA	13543.31	11230.96	52.96847	34.57

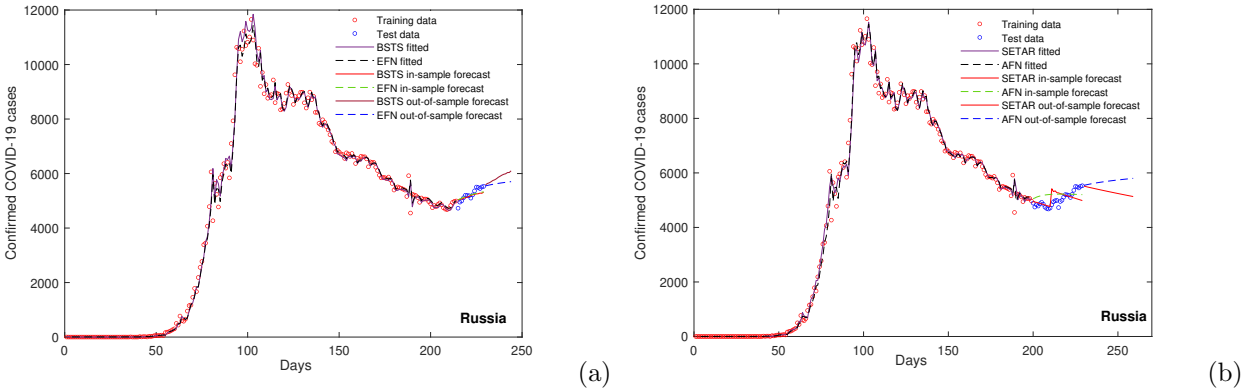

Fig. 7 Plots of (a) 15-days ahead forecast results for Russia COVID-19 data obtained using BSTS and ETS-Theta-ARNN (EFN) models and (b) 30-days ahead forecast results from SETAR and ARIMA-Theta-ARNN (AFN) models.

5.4.5 Results for Peru COVID-19 data

WARIMA and ARFIMA(2,0.09,1) perform better than other single models for 15-days ahead forecasts in Peru. Hybrid WARIMA-ARNN model improves the WARIMA forecasts and has the best accuracy among all hybrid/ensemble models (see Table 16). In-sample and out-of-sample forecasts obtained from WARIMA and hybrid WARIMA-ARNN models are depicted in Fig. 8(a). ARFIMA(2,0,0) and ANN depict competitive accuracy metrics for 30-days ahead forecasts among single forecasting models for Peru COVID-19 data. Ensemble ANN-ARNN-WARIMA (AAW) model has the best accuracy among all hybrid/ensemble models (see Table 17). In-sample and out-of-sample forecasts obtained from ARFIMA(2,0,0) and ensemble AAW models are depicted in Fig. 8(b).

Table 14 Performance metrics with 15 days-ahead test set for Russia

Model	15-days ahead forecast			
	RMSE	MAE	MAPE	SMAPE
ARIMA(0,2,3)	307.34	260.18	4.87	5.02
ETS(A,Ad,N)	215.43	178.64	3.36	3.42
SETAR	436.81	383.72	7.19	7.52
TBATS	215.61	178.79	3.36	3.42
Theta	186.06	157.30	2.97	3.01
ANN	367.19	313.66	5.87	6.09
ARNN(3,2)	208.58	184.74	3.61	3.52
WARIMA	568.44	499.58	9.35	9.92
BSTS	**160.18**	**132.28**	**2.51**	**2.53**
ARFIMA(1,0.1,0)	351.12	297.92	5.57	5.77
Hybrid ARIMA-ANN	308.49	261.17	4.89	5.03
Hybrid ARIMA-ARNN	245.84	207.72	3.92	3.99
Hybrid ARIMA-WARIMA	299.14	251.59	4.72	4.85
Hybrid WARIMA-ANN	489.38	425.98	7.98	8.38
Hybrid WARIMA-ARNN	542.01	473.94	8.87	9.38
Ensemble ARIMA-ETS-Theta	234.64	195.71	3.68	3.75
Ensemble ARIMA-ETS-ARNN	168.14	135.34	2.57	2.59
Ensemble ARIMA-Theta-ARNN	192.28	158.52	2.99	3.03
Ensemble ETS-Theta-ARNN	**157.25**	**127.98**	**2.44**	**2.45**
Ensemble ANN-ARNN-WARIMA	288.26	243.69	4.57	4.69

Table 15 Performance metrics with 30 days-ahead test set for Russia

Model	30-days ahead forecast			
	RMSE	MAE	MAPE	SMAPE
ARIMA(1,2,1)	732.12	546.87	10.40	11.44
ETS(A,Ad,N)	337.44	264.40	5.08	5.25
SETAR	**285.41**	**217.23**	**4.25**	**4.24**
TBATS	337.78	264.62	5.08	5.25
Theta	327.46	297.91	6.04	5.82
ANN	460	340.96	6.48	6.86
ARNN(3,2)	727.63	693.61	13.98	12.97
WARIMA	961.24	727.34	13.86	15.73
BSTS	686.06	509.87	9.79	10.59
ARFIMA(1,0.01,0)	303.35	239.76	4.63	4.74
Hybrid ARIMA-ANN	734.05	548.49	10.43	11.48
Hybrid ARIMA-ARNN	715.58	536.69	10.22	11.19
Hybrid ARIMA-WARIMA	729.96	549.97	10.47	11.5
Hybrid WARIMA-ANN	1012.61	772.11	14.73	16.82
Hybrid WARIMA-ARNN	939.26	715.72	13.65	15.41
Ensemble ARIMA-ETS-Theta	324.95	257.24	4.96	5.10
Ensemble ARIMA-ETS-ARNN	330.79	280.85	5.51	5.56
Ensemble ARIMA-Theta-ARNN	**299.50**	**264.55**	**5.36**	**5.22**
Ensemble ETS-Theta-ARNN	337.63	293.23	6	5.77
Ensemble ANN-ARNN-WARIMA	399.84	324.34	6.29	6.46

Table 16 Performance metrics with 15 days-ahead test set for Peru

Model	15-days ahead forecast			
	RMSE	MAE	MAPE	SMAPE
ARIMA(1,1,1) with drift	2275.49	1686.84	49.97	28.99
ETS(M,A,N)	1689.96	1189.05	31.89	23.15
SETAR	1935.78	1286.56	41.57	23.71
TBATS	1944.26	1301.07	41.72	24.06
Theta	1831.88	1146.27	38.37	21.92
ANN	1771.59	1211.24	38.89	22.75
ARNN(15,8)	2564.65	2244.78	57.13	35.78
WARIMA	**1659.24**	1060.67	**35.22**	20.85
BSTS	1740.18	1082.16	36.48	21.07
ARFIMA(2,0.09,1)	1712.47	**1022.55**	35.65	**20.13**
Hybrid ARIMA-ANN	2189.18	1596.80	47.93	27.96
Hybrid ARIMA-ARNN	1646.88	1244.03	34.95	23.43
Hybrid ARIMA-WARIMA	2082.15	1385.87	43.93	24.99
Hybrid WARIMA-ANN	1560.68	1206.92	34.11	23.43
Hybrid WARIMA-ARNN	**1121.10**	**827.90**	**23.33**	**17.46**
Ensemble ARIMA-ETS-Theta	1677.24	1040.93	35.50	20.46
Ensemble ARIMA-ETS-ARNN	1748.39	1185.23	38.18	22.48
Ensemble ARIMA-Theta-ARNN	1801.56	1324.73	39.97	24.39
Ensemble ETS-Theta-ARNN	1613.15	1048.04	34.76	20.62
Ensemble ANN-ARNN-WARIMA	1864.99	1329.83	41.16	24.43

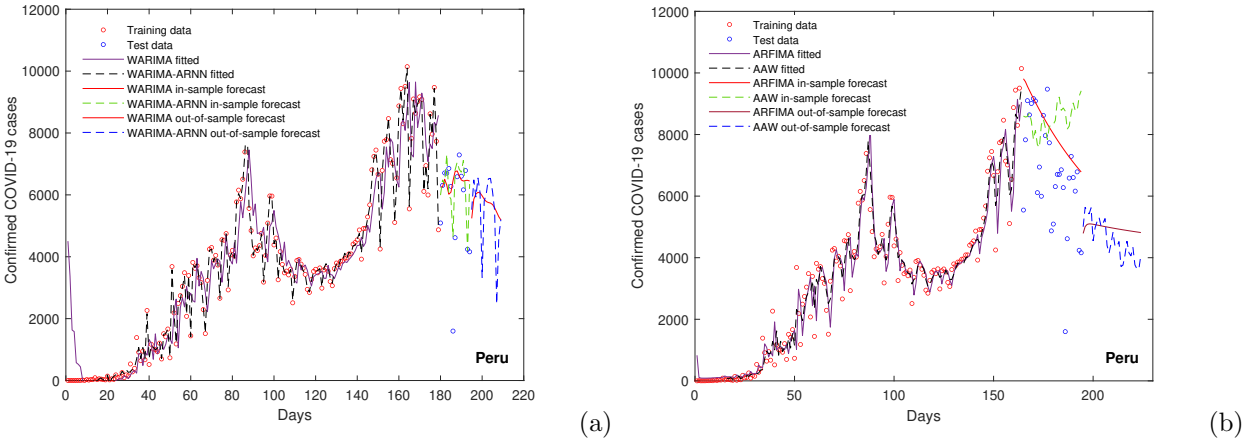

Fig. 8 Plots of (a) 15-days ahead forecast results for Peru COVID-19 data obtained using WARIMA and hybrid WARIMA-ARNN models and (b) 30-days ahead forecast results from ARFIMA and ensemble ANN-ARNN-WARIMA (AAW) models.

Results from all the five datasets reveal that none of the forecasting models performs uniformly, and therefore, one should be carefully select the appropriate forecasting model while dealing with COVID-19 datasets.

6 Discussions

In this study, we assessed several individuals and combined statistical learning models on the confirmed cases of COVID-19 data sets for the five countries, namely the USA, India, Brazil, Russia, and Peru. These COVID-19 daily cases datasets mostly exhibit nonlinear

Table 17 Performance metrics with 30 days-ahead test set for Peru

Model	30-days ahead forecast			
	RMSE	MAE	MAPE	SMAPE
ARIMA(1,1,1) with drift	3889.85	3288.04	70.17	41.92
ETS(M,A,N)	7881.14	6892.41	81.37	66.91
SETAR	4598.98	4077.59	83.67	48.90
TBATS	2924.92	2366.84	52.90	33.13
Theta	3862.84	3374.84	70.68	42.93
ANN	2183.98	1818.07	**30.57**	32.12
ARNN(15,8)	2833.39	2339.49	49.10	32.92
WARIMA	5579.69	4840.75	89.04	54.14
BSTS	5422.13	4851.34	87.98	54.82
ARFIMA(2,0,0)	**2052.01**	**1513.62**	35.37	**23.27**
Hybrid ARIMA-ANN	3756.5	3131.88	67.50	40.46
Hybrid ARIMA-ARNN	4137.45	3619.54	74.50	44.93
Hybrid ARIMA-WARIMA	4164.69	3602.27	75.52	44.78
Hybrid WARIMA-ANN	6372.936	5722.291	95.95	60.80
Hybrid WARIMA-ARNN	5563.043	4819.09	93.16	53.97
Ensemble ARIMA-ETS-Theta	5176.14	4518.43	92.73	51.99
Ensemble ARIMA-ETS-ARNN	4908.85	4153.58	87.26	48.69
Ensemble ARIMA-Theta-ARNN	3410.39	2785.71	61.39	37.11
Ensemble ETS-Theta-ARNN	4826.01	4048.24	85.09	47.82
Ensemble ANN-ARNN-WARIMA	**2626.8**	**2003.06**	**47.02**	**29.02**

and nonstationary behavior. Twenty forecasting models were applied to five datasets, and an empirical comparison is presented here. All five different countries, except Brazil and Peru, will face a diminishing trend in the number of new confirmed cases of the COVID-19 pandemic. Based on the short-term out of sample forecasts reported in this study, the lockdown and shutdown periods can be adjusted accordingly to handle the uncertain and vulnerable situations of the COVID-19 pandemic. Authorities and health care can modify their planning in stockpiles and hospital-beds, depending on these COVID-19 pandemic forecasts.

The empirical findings suggest no universal method exists that can outperform every other model for all the datasets in COVID-19 nowcasting. Still, the future forecasts obtained from models with the best accuracy will be useful in decision and policy makings for government officials and policymakers to allocate adequate health care resources for the coming days in responding to the crisis. However, we recommend updating the datasets regularly and comparing the accuracy metrics to obtain the best model. As this is evident from this empirical study that no model can perform consistently as the best forecasting model, one must update the datasets regularly to generate useful forecasts. Time series of epidemics can oscillate heavily due to various epidemiological factors, and these fluctuations are challenging to be captured adequately for precise forecasting.

7 Conclusion and Future Challenges

In this research, we have focused on analyzing the nature of the COVID-19 time series data and understanding the data characteristics of the time series. This empirical work studied a wide range of statistical forecasting methods and machine learning algorithms. We have also presented more systematic representations of single, ensemble, and hybrid approaches available for epidemic forecasting. This quantitative study could be used to assess the

COVID-19 confirmed case forecasts and will benefit epidemiologists and modelers working on COVID-19 forecasting and modeling.

Considering the scope of this study, we present a set of challenges of pandemic forecasting (short-term) with the available forecasting tools presented in this chapter. To obtain better out-of-sample forecasts of daily COVID-19 cases, it is necessary to (a) collect more data on the factors that contribute to daily confirmed cases of COVID-19; (b) model the entire predictive distribution, with particular focus on accurately quantifying uncertainty (Holmdahl and Buckee, 2020); and (c) continuously monitor the performance of any model against real data and either re-adjust or discard models based on accruing evidence. It is confirmed from the experimental study that there is no universal model that can generate 'best' short-term forecasts of COVID-19 confirmed cases. Epidemiological estimates and compartmental models can be useful for long-term pandemic trajectory prediction, but they often assume some unrealistic assumptions (Ioannidis et al, 2020). Thus, future research is needed to collect, clean, and curate data and develop a coherent approach to evaluate the suitability of models with regard to COVID-19 predictions and forecast uncertainties.

Data and codes

For the sake of repeatability and reproducibility of this study, all codes and data sets are made available at `https://github.com/indrajitg-r/Forecasting-COVID-19-cases`.

References

Aleta A, Martin-Corral D, y Piontti AP, Ajelli M, Litvinova M, Chinazzi M, Dean NE, Halloran ME, Longini Jr IM, Merler S, et al (2020) Modeling the impact of social distancing, testing, contact tracing and household quarantine on second-wave scenarios of the covid-19 epidemic. medRxiv

Aminghafari M, Poggi JM (2007) Forecasting time series using wavelets. International Journal of Wavelets, Multiresolution and Information Processing 5(05):709–724

Anastassopoulou C, Russo L, Tsakris A, Siettos C (2020) Data-based analysis, modelling and forecasting of the covid-19 outbreak. PloS one 15(3):e0230405

Anderson RM, Anderson B, May RM (1992) Infectious diseases of humans: dynamics and control. Oxford university press

Annas S, Pratama MI, Rifandi M, Sanusi W, Side S (2020) Stability analysis and numerical simulation of seir model for pandemic covid-19 spread in indonesia. Chaos, Solitons & Fractals 139:110072

Antonio FDN, Hegger HK, Schreiber T, Di Narzo MAF (2013) Package 'tserieschaos'. dimension 1

Armstrong JS (2001) Principles of forecasting: a handbook for researchers and practitioners, vol 30. Springer Science & Business Media

Assimakopoulos V, Nikolopoulos K (2000) The theta model: a decomposition approach to forecasting. International journal of forecasting 16(4):521–530

Bates JM, Granger CW (1969) The combination of forecasts. Journal of the Operational Research Society 20(4):451–468

Baud D, Qi X, Nielsen-Saines K, Musso D, Pomar L, Favre G (2020) Real estimates of mortality following covid-19 infection. The Lancet infectious diseases

Benettin G, Galgani L, Giorgilli A, Strelcyn JM (1980) Lyapunov characteristic exponents for smooth dynamical systems and for hamiltonian systems; a method for computing all of them. part 1: Theory. Meccanica 15(1):9–20

Black R, Hurst H, Simaika Y (1965) Long-term storage: an experimental study. Constable

Borchers HW, Borchers MHW (2019) Package 'pracma'

Bordley RF (1982) The combination of forecasts: a bayesian approach. Journal of the operational research society 33(2):171–174

Box GE, Pierce DA (1970) Distribution of residual autocorrelations in autoregressive-integrated moving average time series models. Journal of the American statistical Association 65(332):1509–1526

Box GE, Jenkins GM, Reinsel GC, Ljung GM (2015) Time series analysis: forecasting and control. John Wiley & Sons

Brady OJ, Gething PW, Bhatt S, Messina JP, Brownstein JS, Hoen AG, Moyes CL, Farlow AW, Scott TW, Hay SI (2012) Refining the global spatial limits of dengue virus transmission by evidence-based consensus. PLoS Negl Trop Dis 6(8):e1760

Brockwell PJ, Davis RA, Fienberg SE (1991) Time series: theory and methods: theory and methods. Springer Science & Business Media

Buczak AL, Baugher B, Moniz LJ, Bagley T, Babin SM, Guven E (2018) Ensemble method for dengue prediction. PloS one 13(1):e0189988

Chakraborty T, Ghosh I (2020) Real-time forecasts and risk assessment of novel coronavirus (covid-19) cases: A data-driven analysis. Chaos, Solitons and Fractals 135

Chakraborty T, Chattopadhyay S, Ghosh I (2019) Forecasting dengue epidemics using a hybrid methodology. Physica A: Statistical Mechanics and its Applications p 121266

Chakraborty T, Bhattacharyya A, Pattnaik M (2020) Theta autoregressive neural network model for covid-19 outbreak predictions. medRxiv

Chatfield C (2000) Time-series forecasting. CRC press

Chatfield C (2016) The analysis of time series: an introduction. Chapman and Hall/CRC

Chen YC, Lu PE, Chang CS, Liu TH (2020) A time-dependent sir model for covid-19 with undetectable infected persons. IEEE Transactions on Network Science and Engineering

Clemen RT (1989) Combining forecasts: A review and annotated bibliography. International journal of forecasting 5(4):559–583

De Gooijer JG, Hyndman RJ (2006) 25 years of time series forecasting. International journal of forecasting 22(3):443–473

De Livera AM, Hyndman RJ, Snyder RD (2011) Forecasting time series with complex seasonal patterns using exponential smoothing. Journal of the American statistical association 106(496):1513–1527

Di Narzo AF, Aznarte JL, Stigler M (2020) Package 'tsdyn'

Emanuel EJ, Persad G, Upshur R, Thome B, Parker M, Glickman A, Zhang C, Boyle C, Smith M, Phillips JP (2020) Fair allocation of scarce medical resources in the time of covid-19

Fanelli D, Piazza F (2020) Analysis and forecast of covid-19 spreading in china, italy and france. Chaos, Solitons & Fractals 134:109761

Faraway J, Chatfield C (1998) Time series forecasting with neural networks: a comparative study using the air line data. Journal of the Royal Statistical Society: Series C (Applied Statistics) 47(2):231–250

Farmer JD (1982) Chaotic attractors of an infinite-dimensional dynamical system. Physica D: Nonlinear Phenomena 4(3):366–393

Farmer JD, Sidorowich JJ (1987) Predicting chaotic time series. Physical review letters 59(8):845

Ferguson N, Laydon D, Nedjati Gilani G, Imai N, Ainslie K, Baguelin M, Bhatia S, Boonyasiri A, Cucunuba Perez Z, Cuomo-Dannenburg G, et al (2020) Report 9: Impact of non-pharmaceutical interventions (npis) to reduce covid19 mortality and healthcare demand

Franses PH, Van Dijk D, et al (2000) Non-linear time series models in empirical finance. Cambridge university press

Garcia C, Sawitzki G (2015) nonlineartseries: nonlinear time series analysis

Ghosh I, Chakraborty T (2020) An integrated deterministic-stochastic approach for forecasting the long-term trajectories of covid-19. medRxiv preprint doi: https://doi org/101101/202005

Goodfellow I, Bengio Y, Courville A, Bengio Y (2016) Deep learning, vol 1. MIT press Cambridge

Granger CW, Joyeux R (1980) An introduction to long-memory time series models and fractional differencing. Journal of time series analysis 1(1):15–29

Granger CW, Ramanathan R (1984) Improved methods of combining forecasts. Journal of forecasting 3(2):197–204

Grasselli G, Pesenti A, Cecconi M (2020) Critical care utilization for the covid-19 outbreak in lombardy, italy: early experience and forecast during an emergency response. Jama 323(16):1545–1546

Groeneveld RA, Meeden G (1984) Measuring skewness and kurtosis. Journal of the Royal Statistical Society: Series D (The Statistician) 33(4):391–399

Guan Wj, Ni Zy, Hu Y, Liang Wh, Ou Cq, He Jx, Liu L, Shan H, Lei Cl, Hui DS, et al (2020) Clinical characteristics of coronavirus disease 2019 in china. New England journal of medicine 382(18):1708–1720

Hanke JE, Reitsch AG, Wichern DW (2001) Business forecasting, vol 9. Prentice Hall New Jersey

Haslett J, Raftery AE (1989) Space-time modelling with long-memory dependence: Assessing ireland's wind power resource. Journal of the Royal Statistical Society: Series C (Applied Statistics) 38(1):1–21

Hastie T, Tibshirani R, Friedman J (2009) The elements of statistical learning: data mining, inference, and prediction. Springer Science & Business Media

He S, Peng Y, Sun K (2020) Seir modeling of the covid-19 and its dynamics. Nonlinear Dynamics pp 1–14

Hegger R, Kantz H, Schreiber T (1999) Practical implementation of nonlinear time series methods: The tisean package. Chaos: An Interdisciplinary Journal of Nonlinear Science 9(2):413–435

Hellewell J, Abbott S, Gimma A, Bosse NI, Jarvis CI, Russell TW, Munday JD, Kucharski AJ, Edmunds WJ, Sun F, et al (2020) Feasibility of controlling covid-19 outbreaks by isolation of cases and contacts. The Lancet Global Health

Holmdahl I, Buckee C (2020) Wrong but useful—what covid-19 epidemiologic models can and cannot tell us. New England Journal of Medicine

Hou C, Chen J, Zhou Y, Hua L, Yuan J, He S, Guo Y, Zhang S, Jia Q, Zhao C, et al (2020) The effectiveness of quarantine of wuhan city against the corona virus disease 2019 (covid-19): A well-mixed seir model analysis. Journal of medical virology

Hu Z, Ge Q, Jin L, Xiong M (2020) Artificial intelligence forecasting of covid-19 in china. arXiv preprint arXiv:200207112

Huang C, Wang Y, Li X, Ren L, Zhao J, Hu Y, Zhang L, Fan G, Xu J, Gu X, et al (2020) Clinical features of patients infected with 2019 novel coronavirus in wuhan, china. The lancet 395(10223):497–506

Hyndman R, Koehler AB, Ord JK, Snyder RD (2008) Forecasting with exponential smoothing: the state space approach. Springer Science & Business Media

Hyndman RJ, Athanasopoulos G (2018) Forecasting: principles and practice. OTexts

Hyndman RJ, Billah B (2003) Unmasking the theta method. International Journal of Forecasting 19(2):287–290

Hyndman RJ, Khandakar Y, et al (2007) Automatic time series for forecasting: the forecast package for R. 6/07, Monash University, Department of Econometrics and Business Statistics ...

Hyndman RJ, Athanasopoulos G, Bergmeir C, Caceres G, Chhay L, O'Hara-Wild M, Petropoulos F, Razbash S, Wang E (2020) Package 'forecast'. Https://cran.r-project.org/web/packages/forecast/forecast

Ioannidis JP, Cripps S, Tanner MA (2020) Forecasting for covid-19 has failed. International journal of forecasting

James G, Witten D, Hastie T, Tibshirani R (2013) An introduction to statistical learning, vol 112. Springer

Jammalamadaka SR, Qiu J, Ning N (2018) Multivariate bayesian structural time series model. The Journal of Machine Learning Research 19(1):2744–2776

Kantz H, Schreiber T (2004) Nonlinear time series analysis, vol 7. Cambridge university press

Khashei M, Bijari M (2010) An artificial neural network (p, d, q) model for timeseries forecasting. Expert Systems with applications 37(1):479–489

Kim HY (2013) Statistical notes for clinical researchers: assessing normal distribution (2) using skewness and kurtosis. Restorative dentistry & endodontics 38(1):52–54

Kissler SM, Tedijanto C, Goldstein E, Grad YH, Lipsitch M (2020) Projecting the transmission dynamics of sars-cov-2 through the postpandemic period. Science 368(6493):860–868

Kourentzes N (2017a) Nnfor: Time series forecasting with neural networks

Kourentzes N (2017b) nnfor: Time series forecasting with neural networks. r package version 0.9. 6

Kucharski AJ, Russell TW, Diamond C, Liu Y, Edmunds J, Funk S, Eggo RM, Sun F, Jit M, Munday JD, et al (2020) Early dynamics of transmission and control of covid-19: a mathematical modelling study. The lancet infectious diseases

Lemke C, Gabrys B (2010) Meta-learning for time series forecasting and forecast combination. Neurocomputing 73(10-12):2006–2016

Lemke C, Budka M, Gabrys B (2015) Metalearning: a survey of trends and technologies. Artificial intelligence review 44(1):117–130

Li Q, Feng W, Quan YH (2020) Trend and forecasting of the covid-19 outbreak in china. Journal of Infection 80(4):469–496

López L, Rodó X (2020) The end of social confinement and covid-19 re-emergence risk. Nature Human Behaviour 4(7):746–755

Makridakis S, Hibon M (1997) Arma models and the box–jenkins methodology. Journal of Forecasting 16(3):147–163

Maleki M, Mahmoudi MR, Wraith D, Pho KH (2020) Time series modelling to forecast the confirmed and recovered cases of covid-19. Travel Medicine and Infectious Disease p 101742

Messina JP, Brady OJ, Scott TW, Zou C, Pigott DM, Duda KA, Bhatt S, Katzelnick L, Howes RE, Battle KE, et al (2014) Global spread of dengue virus types: mapping the 70 year history. Trends Microbiol 22(3):138–146

Meyer D, Dimitriadou E, Hornik K, Weingessel A, Leisch F, Chang CC, Lin CC, Meyer MD (2019) Package 'e1071'. The R Journal

Montero-Manso P, Athanasopoulos G, Hyndman RJ, Talagala TS (2020) Fforma: Feature-based forecast model averaging. International Journal of Forecasting 36(1):86–92

Mood AM (1950) Introduction to the Theory of Statistics. McGraw-hill

Mosleh A, Apostolakis G (1986) The assessment of probability distributions from expert opinions with an application to seismic fragility curves. Risk analysis 6(4):447–461

Mossong J, Hens N, Jit M, Beutels P, Auranen K, Mikolajczyk R, Massari M, Salmaso S, Tomba GS, Wallinga J, et al (2008) Social contacts and mixing patterns relevant to the spread of infectious diseases. PLoS Med 5(3):e74

Nury AH, Hasan K, Alam MJB (2017) Comparative study of wavelet-arima and wavelet-ann models for temperature time series data in northeastern bangladesh. Journal of King Saud University-Science 29(1):47–61

Paul RK, Samanta S, Paul MRK, LazyData T (2017) Package 'waveletarima'. Seed 500:1–5

Percival DB, Walden AT (2000) Wavelet methods for time series analysis, vol 4. Cambridge university press

Petersen E, Koopmans M, Go U, Hamer DH, Petrosillo N, Castelli F, Storgaard M, Al Khalili S, Simonsen L (2020) Comparing sars-cov-2 with sars-cov and influenza pandemics. The Lancet infectious diseases

Peterson BG, Carl P, Boudt K, Bennett R, Ulrich J, Zivot E, Cornilly D, Hung E, Lestel M, Balkissoon K, et al (2018) Package 'performanceanalytics'. R Team Cooperation

Petropoulos F, Makridakis S (2020) Forecasting the novel coronavirus covid-19. PloS one 15(3):e0231236

Philemon MD, Ismail Z, Dare J (2019) A review of epidemic forecasting using artificial neural networks. International Journal of Epidemiologic Research 6(3):132–143

Phillips PC, Perron P (1988) Testing for a unit root in time series regression. Biometrika 75(2):335–346

Pumi G, Valk M, Bisognin C, Bayer FM, Prass TS (2019) Beta autoregressive fractionally integrated moving average models. Journal of Statistical Planning and Inference 200:196–212

Rajgor DD, Lee MH, Archuleta S, Bagdasarian N, Quek SC (2020) The many estimates of the covid-19 case fatality rate. The Lancet Infectious Diseases 20(7):776–777

Ray D, Salvatore M, Bhattacharyya R, Wang L, Du J, Mohammed S, Purkayastha S, Halder A, Rix A, Barker D, et al (2020) Predictions, role of interventions and effects of a historic national lockdown in india's response to the covid-19 pandemic: data science call to arms. Harvard data science review 2020(Suppl 1)

Ribeiro MHDM, da Silva RG, Mariani VC, dos Santos Coelho L (2020) Short-term forecasting covid-19 cumulative confirmed cases: Perspectives for brazil. Chaos, Solitons & Fractals p 109853

Robinson PM (1995) Log-periodogram regression of time series with long range dependence. The annals of Statistics pp 1048–1072

Roosa K, Lee Y, Luo R, Kirpich A, Rothenberg R, Hyman J, Yan P, Chowell G (2020) Real-time forecasts of the covid-19 epidemic in china from february 5th to february 24th, 2020. Infectious Disease Modelling 5:256–263

Rosenbaum L (2020) Facing covid-19 in italy—ethics, logistics, and therapeutics on the epidemic's front line. New England Journal of Medicine 382(20):1873–1875

Rosenstein MT, Collins JJ, De Luca CJ (1993) A practical method for calculating largest lyapunov exponents from small data sets. Physica D: Nonlinear Phenomena 65(1-2):117–134

Rumelhart DE, Hinton GE, Williams RJ (1985) Learning internal representations by error propagation. Tech. rep., California Univ San Diego La Jolla Inst for Cognitive Science

Scott SL, Varian HR (2013) Bayesian variable selection for nowcasting economic time series. Tech. rep., National Bureau of Economic Research

Scott SL, Varian HR (2014) Predicting the present with bayesian structural time series. International Journal of Mathematical Modelling and Numerical Optimisation 5(1-2):4–23

Scott SL, Scott MSL, Scott MS, BoomSpikeSlab D, Boom L (2020) Package 'bsts'

Shaub D (2020) Fast and accurate yearly time series forecasting with forecast combinations. International Journal of Forecasting 36(1):116–120

Shaub D, Ellis P (2019) forecasthybrid: Convenient functions for ensemble time series forecasts. R package: https://CRAN R-project org/package=forecastHybrid 4(17):238

Shin Y, Schmidt P (1992) The kpss stationarity test as a unit root test. Economics Letters 38(4):387–392

Smith J, Wallis KF (2009) A simple explanation of the forecast combination puzzle. Oxford Bulletin of Economics and Statistics 71(3):331–355

Spiliotis E, Assimakopoulos V, Makridakis S (2020) Generalizing the theta method for automatic forecasting. European Journal of Operational Research 284(2):550–558

Sujath R, Chatterjee JM, Hassanien AE (2020) A machine learning forecasting model for covid-19 pandemic in india. Stochastic Environmental Research and Risk Assessment p 1

Teräsvirta T, Lin CF, Granger CW (1993) Power of the neural network linearity test. Journal of time series analysis 14(2):209–220

Teräsvirta T, Van Dijk D, Medeiros MC (2005) Linear models, smooth transition autoregressions, and neural networks for forecasting macroeconomic time series: A reexamination. International Journal of Forecasting 21(4):755–774

Timmermann A (2006) Forecast combinations. handbook of economic forecasting

Tong H (1990) Non-linear time series: a dynamical system approach. Oxford University Press

Tong H (2002) Nonlinear time series analysis since 1990: Some personal reflections. Acta Mathematicae Applicatae Sinica 18(2):177

Trapletti A, Hornik K, LeBaron B (2007) tseries: Time series analysis and computational finance. R package version 010-11

Trilla A, Trilla G, Daer C (2008) The 1918 “spanish flu” in spain. Clinical infectious diseases 47(5):668–673

Tsay RS (1986) Nonlinearity tests for time series. Biometrika 73(2):461–466

Tsay RS (2000) Time series and forecasting: Brief history and future research. Journal of the American Statistical Association 95(450):638–643

Wang Ws (2002) Multiple time scales analysis of hydrological time series with wavelet transform. Journal of Sichuan University: Engineering Science Edition 34(6):14–17

Wang X, Smith-Miles K, Hyndman R (2009) Rule induction for forecasting method selection: Meta-learning the characteristics of univariate time series. Neurocomputing 72(10-12):2581–2594

Weinberger DM, Cohen T, Crawford FW, Mostashari F, Olson D, Pitzer VE, Reich NG, Russi M, Simonsen L, Watkins A, et al (2020) Estimating the early death toll of covid-19 in the united states. bioRxiv

Winters PR (1960) Forecasting sales by exponentially weighted moving averages. Management science 6(3):324–342

Wolpert DH, Macready WG (1997) No free lunch theorems for optimization. IEEE Trans Evol Comput 1(1):67–82

Wu JT, Leung K, Leung GM (2020) Nowcasting and forecasting the potential domestic and international spread of the 2019-ncov outbreak originating in wuhan, china: a modelling study. The Lancet 395(10225):689–697

Zhang G, Patuwo BE, Hu MY (1998) Forecasting with artificial neural networks:: The state of the art. International journal of forecasting 14(1):35–62

Zhang GP (2003) Time series forecasting using a hybrid arima and neural network model. Neurocomputing 50:159–175

Zhang GP, Qi M (2005) Neural network forecasting for seasonal and trend time series. European journal of operational research 160(2):501–514

Zhuang Z, Cao P, Zhao S, Lou Y, Wang W, Yang S, Yang L, He D (2020) Estimation of local novel coronavirus (covid-19) cases in wuhan, china from off-site reported cases and population flow data from different sources. medRxiv